PREPARATION, CHARACTERIZATION AND CATALYTIC TESTING OF MONO- OR BIMETALLIC ZEOLITE CATALYSTS IN C-Cl BOND CLEVEAGE REACTION

Ph.D. THESIS

TAMÁSI ANIKÓ

UNIVERSITY OF SZEGED
DEPARTMENT OF APPLIED AND ENVIRONMENTAL CHEMISTRY
SZEGED
2001

Supervisor:
Prof. Imre Kiricsi

1. INTRODUCTION

Over the past few years, the community of chemists has been mobilized to find new reactions and develop new products that are less hazardous to human health and environment. These new approaches, which have received extensive attention and go by many names including Green Chemistry, Environmentally Benign Chemistry, Clean Chemistry, include new synthetic methods and processes as well as new tools for instructing aspiring chemists how to do chemistry in a more environmentally benign manner.

There is no doubt that over the past 20 years, the chemists and chemical engineers have made extensive efforts to reduce the risk associated with the manufacture and use of various chemicals. Innovative chemistries have been developed to treat chemical wastes and remediate hazardous waste sites. New monitoring and analytical tools have been applied for detecting contamination in air, water and soils. New handling procedures and containment technologies have been standardized to minimize exposure. While these areas are laudable efforts in the reduction of risk, they do not prevent pollution, but rather they are for pollution control.

Elimination of wastes is the first goal of environmentally friendly processing, the second is the reduction of dependence on the use of hazardous chemicals. The key achieving these goals is, in many cases, to substitute a catalytic for a stoichiometric process. Selective catalytic reactions often enable by-products and waste to be reduced or eliminated. Catalytic hydrogenation can in many cases replace reduction with metals or hydrides, catalytic oxidation with molecular oxygen or H_2O_2 can eliminate the need for stoichiometric oxidants, and solid acids may provide an alternative to aluminum chloride and acids such as HCl, HF and H_2SO_4. Catalysis can also lead to reduction in the number of process steps and the use of milder processing conditions.

Both homogenous and heterogeneous catalysis find wide-ranging application in production of chemicals. Heterogeneous catalysis generally offers the advantage of simple separation and recovery, can be employed for both gas- and liquid-phase reactions, and lend themselves for continuous reactor operations.

The advantages of heterogeneous catalysis were first appreciated in the petroleum refining and bulk chemical industries.

The possibilities offered by zeolites for introducing metal functions and for tuning such essential catalytic properties as hydrophyilicity/hydrophobicity balance and the type and strength of acid sites make them widely applicable as catalytic materials. Nowadays, the utilization of zeolites in environmental friendly processes gains ground extensively; they are used as ion-exchange agents in phosphate free washing powders, as adsorbents to attract and hold H_2S or NO_x from industrial exhaust gases and as catalysts as well.

One of the catalytic processes where zeolites can be applied is the C-Cl bond cleavage reaction. Chlorinated organic compounds are considered to be harmful environmental pollutants. Examples include chlorinated and brominated aromatic hydrocarbons that are environmentally hazardous chemicals, which threaten human health and other biological systems; and chloroflourocarbons (CFCs) that are known to destroy ozone in the stratosphere. The desirable solution to eliminate these compounds is to convert them to less harmful chemicals, which can be applied as reagents for fine chemical processes. If this is not feasible it is important to arrange their total decomposition.

The catalytic science community looks for the answers to solve these problems for a long time. However, during technological realization new problems and open questions arise, which can be the basis of further investigations.

2. REVIEW OF LITERATURE

2.1. Zeolites

Zeolites are well-defined class of crystalline aluminum hydrosilicates. They have three-dimensional structures built up from tetrahedral units linked *via* common oxygen atoms. These units, in which either Si or Al are sitting in their centers, form cages and channels of molecular dimensions (see Figure 1). The presence of $(AlO_2)^-$ units causes residual negative charge on the oxygen framework. These negative charges are compensated by the cations located in the pores bounded to aluminum by electrostatic forces assuring their easy exchange for other ions. The cavities and channels of zeolites are filled with water in their hydrated form. The number and location of H_2O molecules depend on the overall architecture of the zeolite, such as the size and shape of the cavities, channels and the number and nature of cations present in the structure. This water can easily be removed by simple heating above 100 °C. [1,2]

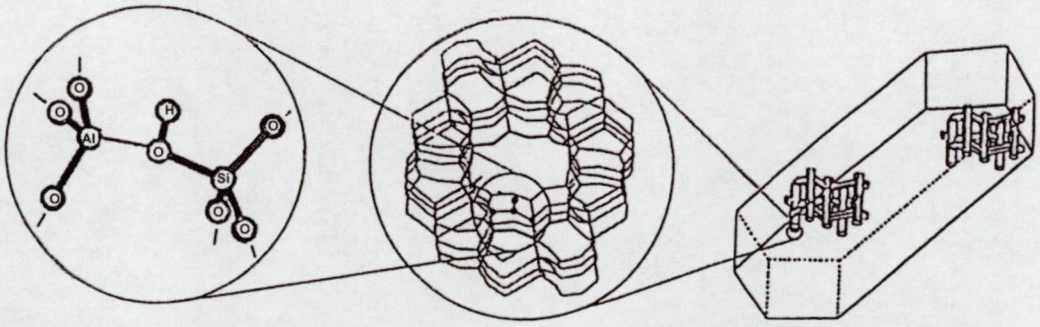

Figure 1. *Structure of ZSM-5 type zeolite*

One possibility to classify zeolite structures is to relate them to the symmetry of their unit cells. This is inconvenient and oversimplified, since different zeolite structures often have identical repeating subunits, being less complex than their unit cells. These represent only the aluminum-silicate skeleton and exclude consideration of water molecules and cations sitting within the cavities and channels of the framework.

Nowadays, 36 types of zeolites can be mined, and hundreds of different synthetic zeolites are registered.

Zeolites have been widely applied in industrial processes as molecular sieves, ion-exchangers, and heterogeneous catalysts [3]. Noncatalytic uses of zeolites of various pore/channel dimensions include selective adsorption in large-scale separation processes. In catalytic applications, zeolites are predominantly used in their acidic form. The most important processes in this category is fluidized catalytic cracking, based on rare earth-exchanged zeolites, mainly X and Y of the faujasite structure with small admixtures of ZSM-5. Another industrial process in this group is catalytic dewaxing using mordenite and ZSM-5. Applications of ZSM-5 and faujasites in synfuel production, isomerization, and other industrially important reactions have been thoroughly reviewed [4]. Ti-substituted zeolites display unique activity in oxidation catalysis [5].

Cu ion containing zeolite supported catalysts was found to be highly efficient in NO_x decomposition [6]. This finding is of great interest in view of the legislative demand to remove NO_x from exhaust emission of vehicles and the stack gas of power plants.

The Cyclar catalyst, which contains Ga in HZSM-5, is used for the dehydrocyclodimerization of propane and butane to benzene and its homologues [7]. The list could be continued since the application of transition or noble metal loaded zeolites gains more and more ground.

The majority of transition metal containing zeolite catalysts is bifunctional, i.e., both strong acid sites and metal components are present in the same zeolites. The traditional model for bifunctional catalysis, introduced by Mills et al. [8], assumes that metal sites mainly provide the hydrogenation and dehydrogenation function, whereas the acid sites catalyze isomerization and cracking reactions. Further, the traditional model accepts a concomitant role of metal, to hydrogenate coke precursors that is, thus preventing the deposition of carbonaceous overlayers. In this model it is often tacitly assumed that a small amount of the platinum metal is sufficient to maintain the paraffin/olefin ratio in the product. It was, however, shown by Ribeiro et al. [9] that the isomerization activity of Pt/HY and Pt/H-mordenite catalysts increases almost linearly with the number of exposed Pt atoms up to a given concentration. The conventional classification of the reaction network into metal-catalyzed (de)hydrogenation acid-catalyzed isomerization and cracking steps is certainly an oversimplification of the reality.

Most recent results cast doubts on the assumption that metal and acid sites have to be geometrically separated one from another, so that reaction intermediates must shuttle between them [10]. New data suggest that metal particles in zeolites can combine with protons to form one entity [11]. As the metal-proton adduct carries a net positive charge, the metal has become "electron deficient" [12].

Zeolites appear to be different from other supports such as amorphous materials, glasses etc. The advantages of their application are as follows [13]:

(i) Geometrical constraint to form well-dispersed metal particles in the nanoscale range;

(ii) Small and uniform particle size associated with
- shape selectivity (selectivity for reactant, for intermediate or for product, which is provided by the molecular dimension channel or cage system of the zeolite),
- acid-base properties (the concentration and strength of which can be significantly controlled by the different preparation methods);

(iii) Electronic interaction of the metal particles with their environments, such as charges in the zeolite cages, resulting in superior catalytic activity compared to conventional oxide supported catalysts.

The disadvantages are:

(i) The migration of the reduced metal components towards the external surface of zeolite upon heat treatment, which may lead to the loss of shape selectivity in a given reaction.

(ii) The agglomerated metal can fill up the pores and/or block the zeolite pore structure.

(iii) Diffusion hindrance might step up in the pores.

However, the unfavorable properties can be largely diminished or eliminated by appropriate catalyst preparation.

2.1.1. Preparation of metal loaded zeolites

Various techniques are available for the introduction of metals into zeolites. Ion-exchange and impregnation are used the most often. The former method introduces only cations into the zeolite, whereas the latter also incorporates an equivalent number of anions. In both cases, the introduction of ions has to be followed by calcination and reduction steps in order to remove H_2O and to transform metal ions to metal. For zeolite-based catalysts the ion-exchange method is preferred [13, 14, 15, 16].

The ion-exchange isotherms for most metal ions and commercial zeolites have been reported [17, 18, 19, 20, 21]. The introduction of transition metal ions by conventional ion-exchange requires special attention. The pH of the slurry has to be adjusted in order to avoid the undesirable hydrolysis of the transition metal ions. Several multivalent ions exist as free cations only in strong acid solution inferring with the zeolite stability. The pH of the washing solvent should be the same as that applied for the ion-exchange, otherwise the ion distribution among the possible cation exchange position may change and metal hydroxide may be formed, which causes differences in reducibility. In the preparation of bimetallic zeolite catalysts by subsequent ion-exchange of the two ions, the pH of each individual exchange step must be carefully performed to meet the designed characteristics of the final catalysts.

A convenient solution to avoid hydrolysis is to use complex ions for ion-exchange. The most frequently applied complexes are the tetramine ($[Pt(NH_3)_4]^{2+}$, $[Pd(NH_3)_4]^{2+}$), hexamine ($[Ru(NH_3)_6]^{3+}$, $[Co(NH_3)_6]^{3+}$) or pentamine-chloride ($[Rh(NH_3)_5Cl]^{3+}$) complexes. The advantage of their use is that they have increased resistance to hydrolysis but still have cationic character. Besides modifying the solubility of metal ions, amine ligands also affect the distribution of the ions in zeolite cages. A study of Zhang et al. [22] shows that Co^{2+} ions that were introduced into NaY as $Co(H_2O)_6^{2+}$ ions can swiftly migrate into sodalite cages after dehydration even at low temperature. However, when $Co(NH_3)_6^{3+}$ precursors are used, autoreduction takes place leading to monoamine-Co^{2+} ions, which remain in the supercages even at elevated temperatures. The

decomposition of the complex ions must be performed very carefully, avoiding the generation of acid sites or the migration of the bare ions into hindered, inaccessible positions in the cage or channel system of the zeolite.

In a few cases, the conventional ion-exchange procedure is not suitable for introducing appropriate amounts of transition metal ions into the zeolites. To overcome this problem, solid-state ion-exchange may be applied [23]. This procedure consists of high temperature heat treatment of an intimate mixture of the zeolite and the metal salt of the entering ions. Using this method, transition and noble metal ions, such as Co^{2+}, Mn^{2+}, Fe^{3+}, V^{4+}, Nb^{5+}, Mo^{5+}, Pt^{2+}, Pd^{2+} and Rh^{3+} and also ion pairs, such as V/Cu, Cr/Cu were successfully introduced into faujasite and ZSM-5 type zeolites.

Metal ions and neutral metal compounds may be introduced into the zeolites by impregnation [14-16]. Both incipient wetness and imbibement techniques are often used. The former method introduces, preferentially, metal cations into the zeolites, while the latter incorporates equivalent amount of anion from the aqueous solution of the salts. These procedures are applied mainly when the influence of anions, which may remain in very low concentration in the zeolite even after severe heat treatment, is negligible. This is never the case when chloride salts are used. Generally, in these methods, the ion-exchange of the cation takes place simultaneously with the impregnation. Exceptions are only the cases when the size of the simple or complex metal ion hinders their pass across the pore openings or when the ion-exchange equilibrium for the given ion-zeolite pair is not favored. From this follows that various moieties may be present in the zeolites prepared by these techniques.

The impregnation method is the sole possibility for the introduction of quite large neutral metal complexes, such as organometallic compounds. Generally, the solvent of the solution containing the metal compound is evaporated slowly under vigorous stirring.

A convenient route for introducing metal components into the zeolite pores is the vapor phase deposition of the appropriate compound. Often, metal carbonyls are introduced into zeolites in this way [24, 25]. The advantages of this procedure are as follows: (i) the volatile metal carbonyls distribute homogeneously in the pores, (ii) after the decomposition of carbonyls, the metal is present in

atomic dispersion and (iii) no reoxidation of the metal takes place since no protons (water) are simultaneously present. The severe reduction conditions can be avoided by starting from an appropriate volatile precursor. The most frequently used carbonyls are $Fe(CO)_5$, $Fe_3(CO)_{12}$, $Fe_2(CO)_9$, $Co(CO)_8$, $Ni(CO)_4$. Iron clusters prepared in this way proved to be active for syngas conversion [26]. It is very difficult, almost impossible, to reduce Mn, W an Cr ions to metal introduced into zeolites in a conventional way, therefore, their carbonyls ($Mn_2(CO)_{10}$, $Cr(CO)_6$, $W(CO)_6$) are used as precursors of the metals.

The alkali metal azides (LiN_3, NaN_3, CsN_3) can be used for the preparation of alkali metal clusters in zeolites (Li/LiY-FAU, Na/NaY-FAU and Cs/CsY-FAU). The corresponding azides are impregnated onto the zeolite from methanol solution, and the sample is decomposed in inert gas stream to produce the metal cluster. It has been shown by 1-butene double bond isomerization and allyl-cyanide transformation reaction that the catalysts prepared by this method has strong basic character [27, 28, 29].

It is worth mentioning that the vapor-phase deposition technique has been applied only for large pore zeolites, particularly for NaX-FAU and NaY-FAU.

The purpose of subsequent calcination step is to remove water and to decompose ligands for $[Pt(NH_3)_4]^{2+}$ ions by the release of NH_3. A secondary effect of calcination is that the metal ions, after being deprived of their ligands, will migrate into smaller zeolite cages, e.g., sodalite cages or hexagonal prisms for NaY-FAU. Of course, if it is not required there are several ways to avoid it [12, 30, 31].

Often, another side effect of calcination is that NH_3 from decomposing groups may reduce the metal ions prematurely. If this "autoreduction" takes place, the metal atoms tend to agglomerate to large particles, which is, of course, undesirable. Very cautious calcination programs have been proposed by Gallezot et al. [32] – very slow (0.5 K/min) heating rate and high oxygen flow rate (2000 ml/min/g) – in order to minimize autoreduction.

Guczi et al. [33] have proved that in the case of bimetallic zeolites pre-treatment conditions affect the acidity of the zeolites beside influencing the location and reducibility of bimetallic particles.

Reduction is generally carried out in a stream of hydrogen. In this procedure, equivalent amounts of protons are generated, as has been described in an early work of Breck et al. [34] and proved by IR spectroscopy [35]. In addition to hydrogen, other reducing agents, such as alkali metal vapor [36], nitrogen oxide [37], aqueous solution of hydrazine hydrochloride or sodium borohydride were also applied [38]. Reduction with carbon monoxide is a peculiar case since upon reduction of the metal ion, CO should be oxidized to CO_2. As no oxygen is present in the system, this oxidation consumes framework oxygen, meanwhile formation of Lewis acid centers takes place [39].

Depending on the metal precursor (i.e., either metal ion in cation-exchange position, or metal oxide and/or metal complexes in the channels and cages), the reduction results in the creation of different ions and/or molecules in addition to finely dispersed metal particles. The difference among the respective species is the largest when transition or noble metal ions in group VIII or metal oxides generated during the pretreatment are reduced with hydrogen. In the former case, protons are generated,

$$M^{2+} + H_2 \rightarrow M^0 + 2\,H^+,$$

while in the latter, water molecules form as reduction products.

$$[PtO]_n + 2n\,H^+ \rightarrow n\,Pt^{2+} + n\,H_2O$$

When water is generated during the reduction of metal oxide particles, water vapor may locally damage the zeolite framework, depending on the reaction temperature [13].

The protons, e.g., interact with the transition or noble metal ion, resulting in the reoxidation of the metal particle associated with hydrogen formation.

$$M^0 + 2\,H^+ \rightarrow M^{2+} + H_2$$

It is generally accepted that the higher the temperature, the higher the mobility of charge compensating cations is. This means that the metal ions migrate into the smaller cages or occupy more hindered positions in zeolite crystals. These ions can be reduced under more severe condition, and the metal formed remains in the small cages, and therefore, it becomes inaccessible for the reactant molecules. The metal atoms generated in the reduction can migrate out of the zeolite channels and cages and form large metal agglomerates on the outer

surface of the zeolite crystals. In several cases, this unwanted effect may be decreased or completely avoided using one of the following measures:

(i) Before introducing the transition or noble metal ions into the zeolite, the ion position in small cages or in hidden positions should be filled with ions exchanged preferentially to these sites. Such ions are magnesium, calcium and strontium [31,40].

(ii) Instead of using simple hydrated ions for exchange, complex ions (generally amine complexes) of the respective transition metal should be used, since these ions are too big to enter the small cages or hidden positions [22]. Consequently, the metal particles generated by reduction also remain in the large cavities, i.e., in the supercage of the faujasite zeolite.

There are several methods for decreasing the temperature applied for reduction. For hydrolized metal ions reduction follows different chemistry at lower temperatures. After ion-exchange the washing process should be performed with alkaline water in order to transform the exchanged ions into hydroxides. In this case calcination is likely to result in the formation of hydroxide or oxide particles. The reduction of these precursors will produce multiatom particles and water vapor. This reduction process has much smaller activation energy compared to the reduction of ion precursors [41, 42]. This method can be applied for the metal ions, which are hardly reducible in the ionic form in the zeolites.

The reduction of less reducible transition metal ions can be significantly enhanced by readily reducible noble metals. When ion pairs are formed between the less reducible metal ions and the ions of noble metals, both ions enhance the reduction of each other, as was found for Pd-Co [22], Pt-Co [43, 44], and Ru-Co [44, 45] ion pairs.

Using $NaBH_4$ in aqueous solution, the formation of protons can be suppressed since sodium ions will be the charge compensation cations.

We can conclude that no uniform reduction procedure that is generally applied exists. The lack of the same implies that extremely great care should be taken to find the optimal experiment condition for reduction.

2.1.2. Bimetallic zeolites

There have been substantial efforts to investigate the structural, electronic and chemical properties of bimetallic systems. Many fundamental studies have been focused on trying to understand the roles of "ensemble" and "ligand" effects in bimetallic catalysts [46]. Ensemble effects are defined in terms of the number of surface atoms needed for a catalytic process to occur. Ligand effects refer to those modifications in catalytic activity or selectivity that are the result of electronic interactions between the components of the bimetallic system. In gathering information to address these questions, it has been advantageous to simplify the problem by utilizing models of bimetallic catalysts, such as the deposition of metals on single crystal substrates in clean environment familiar to surface science. These well-defined bimetallic surfaces have offered unique possibility to correlate surface chemical reactivity with atomic level surface structure.

Formation of stable bimetallic particles or alloys is prerequisite for improved catalytic properties in several reactions. The effect of the second metal component can be different:

(i) The second metal may be used to dilute the first introduced metal component, in order to increase dispersion and avoid aggregation of the noble metal and to decrease the deactivation effect of the catalyst. For instance, the bimetallic Pd-Pt H-Beta and USY zeolites are found to be more active and selective in isomerization of heptane compared to Pt or Pd loaded derivatives [47]. The dispersion of platinum is significantly improved in the presence of 20 mole % palladium. The improved Pt dispersion leads to better intimacy and balance of the acidic and hydrogenation-dehydrogenation functions in these bifunctional catalysts. Furthermore, the undesirable hydrogenolysis and dimerization-cracking activity of the catalyst are suppressed as well.

(ii) The presence of reducible ions can enhance the reduction of hardly reducible transition metal ions. It has been shown by temperature programmed reduction (TPR) that Co^{2+} or Fe^{3+} ions are almost irreducible in zeolite cages below 770 K. However, in the presence of noble metal

components (Pd or Pt) the reduction can be performed below 770 K, since the activation energy of reduction has been lowered [14- 16, 22, 43-45].

(iii) The two metals present in the zeolitic cages can form alloy particles. In many cases the catalytic activity and/or selectivity of bimetallic catalysts are favorably increased in a given reaction compared to those for the monometallic representatives. By alloy formation the chemisorption properties of the metals and this way the mechanism of the reaction may change significantly. Pt-Mo bimetallic catalysts supported on Y-FAU zeolite exhibit enhanced hydrogenolysis activity with respect to PtY-FAU zeolite in butane conversion [25]. The activity vs. Pt/Mo composition curve is volcano-shaped with a maximum near equiatomic composition. The kinetic parameters are interpreted in terms of the participation of both Pt and Mo atoms in the reaction mechanism. Mo atoms act primarily as strong adsorption sites for the hydrocarbon molecules whereas hydrogen atoms dissociated on Pt are required to hydrogenate the hydrocarbon fragments.

It seems even more important when metal particles are entrapped inside the zeolite cages or channels. Zeolites proved to be remarkably different from oxide supports. Hexane reforming activity of Pt(0.5)Ir(0.5)/Al_2O_3 and Pt(0.5)Ir(0.5)/HY have been compared [48]. The bimetallic catalysts are not subjected to severe oxidative agglomeration and their activity and selectivity are different from those of platinum and iridium monometallic catalysts. HY-FAU zeolite-supported catalysts have higher yields for isomers and lower yields for light hydrocarbons and benzene than the alumina-supported catalysts. This is good characteristic of reforming catalysts for production of high-octane reformate containing less aromatic compound.

Bimetallic zeolite catalysts have been widely used in heterogeneous catalysis. One of the major applications is in the catalytic reforming of refinery naphtha. Namely, Pt-Pd/H-Beta and Pt-Pd/USY have been studied for heptane hydrocracking reaction [47], Pt-Sn or In/NaY-FAU for propane dehydrogenation and hexane cyclization [49]. Pt-Ir/HY-FAU catalysts showed high activity in hexane isomerisation [48], while Pt-Mo/NaY in butane hydrogenolysis reaction [25].

The investigation of Fischer-Tropsch catalyst is the other potential field of application of bimetallic zeolites. Numerous papers including extended reviews

deal with this topic [13-16,22,43-45,50]. According to the different types of catalysts used the product distribution change significantly. For producing CH_4 from CO + H_2 Ru-Ni/NaY-FAU [50] or Pd-Co/NaY-FAU [22, 51] are offered with high efficiency. Oxygenates, such as different alcohols, can be obtained using Pt-Co/NaY catalyst [14-16, 43-45]. Ru-Co/NaY-FAU is reported to produce high molar weight products with low olefin/paraffin ratio. Since the bimetallic particles are inside the zeolite pores and the olefin species have a longer residence time before leaving for the gas phase, their hydrogenation takes place to a higher extent.

Recently, research on ZSM-5 type zeolite supported bimetallic systems is expanded. Cu-ZnZSM-5 is proposed for water gas shift reaction [52], Pt-CuZSM-5 for hydrogenation, isomerisation and hydrocracking reaction [53], while Pt-CoZSM-5 seems to be promising in NO_x selective catalytic reduction by propene [54, 55] or methane [56, 57].

The alloys of platinum-copper and platinum-cobalt, which we have chosen to investigate and apply, have been frequently studied to elucidate the alloying effects in adsorption and catalysis [14-16, 22, 53, 58]. Many parallels can be drawn between the formation and properties of the two systems, but differences can be shown as well.

The structure and growth mode of bimetallic Pt-Cu particles in NaY-FAU were demonstrated by Sachtler et al. [58, 59]. During the reduction Pt particles form first and act as nucleation sites for the Cu atoms leaving the sodalite cages. After their adsorption and reduction the platinum particles would be covered with copper atoms, but subsequent reconstruction to the energetically most favorable atomic arrangement brings Pt atoms to the surface of the particle again. Finally the composition of alloy tends towards a 40:60 ratio for Cu:Pt on the surface, while the interior of the particle may vary within wide limits.

In the case of Pt-Co/NaY-FAU system bimetallic particles do not form if the Co ions are located in the sodalite cages. Both cations have to be present in the supercages for alloy formation, and the reduction step has to be performed carefully. The existence of bimetallic alloy can be disclosed by observing the changes in the infra red (IR) frequencies of adsorbed CO. The red shift caused by Co addition to Pt/NaY-FAU for linearly bound CO at room temperature can be

attributed to electronic interaction between Pt and Co. The +0.5 eV shift in Co 2p binding energy measured by X-ray photoelectron spectroscopy (XPS) verifies the finding [60]. The Pt-Co alloy has a sandwich structure, in which the outmost atomic layer consists of Pt and a second layer enriched in Co.

The Si/Al ratio of ZSM-5 is much higher than that is for NaY-FAU, thus its ion-exchange capacity is lower, but the thermal-stability is higher than those of the faujasite zeolite are. In Pt-CuZSM-5 the electron micrographs reveal highly dispersed metal particles with narrow particle size distribution [53]. Only a small number of larger metal aggregates can be found on the external surface. Alloy formation between copper and platinum have been detected by Fourier transformed infrared (FT-IR) and extended X-ray Absorption Fine Structure (EXAFS) spectroscopic methods, even though Pt-Cu alloy belongs to the weakly exothermic alloys, consequently, the bonding is weak and individual components preserve their identities. Results obtained from CO adsorption measurements are explained on the basis of predominating electronic influences. Ligand effect leads to stronger back-donation of electronic charge to the $2\pi^*$ orbital of the CO. The narrowing of the Pt d band in the alloy and the preferential interaction of the CO $2\pi^*$ orbital with s orbitals of the Pt surface results in an unusual high integral intensity for bridge-bonded CO. The additional geometric influence is due to the dilution of the Pt surface. High resolution electron microscopy (HREM) combined with energy-dispersive X-ray microanalysis (EDX) of the Pt-CoZSM-5 catalyst revealed the existence of particles containing both Co and Pt, while highly dispersed and large Co particles were detected as well [56]. After activation Pt is reduced, while Co stays in an oxidic state.

The bimetallic particles behave differently in zeolite matrix compared to oxide hosts, because of the appearance of acid centers occurring during the reduction step if hydrogen is used as reducing agent. A part of copper or cobalt atoms on the surface of Pt-Cu or Pt-Co particles can be reoxidized, even under mild oxidative conditions. The oxidized copper or cobalt ion leaves the alloy particle, resulting in the segregation of the bimetallic particle. On one hand this segregation can be reversed by re-reduction of the Pt-Cu zeolite, however on the other hand once Co leaches out form Pt-Co bimetallic particles, it will migrate to

hindered positions where reduction can only occur at much higher temperature [53, 61].

2.2. Characterization of zeolites

The first step, that has to be made for characterization, is to determine the composition of the zeolite. After decomposition the exact bulk composition can be measured by Atomic Absorption Spectroscopy (AAS) or Inductively Coupled Plasma Atomic Emission spectroscopy (ICP-AES) or classical analytical methods. X-ray Fluorescence Spectroscopy (XRF) is also applicable without destruction of the sample if the adequate standards are available. To determine the surface concentration X-ray Photoelectron Spectroscopy (XPS) can be used.

The structure of the zeolites can be checked by X-ray or Electron Diffraction (XRD or ED) methods. The diffraction pattern is different for each zeolite and the intensities of the lines are in correlation with the degree of crystallization. The measured diffraction patterns can be compared to the diffractograms found in databases or in atlases of zeolites [62].

IR Spectroscopy (KBr technique) is a sensitive method to investigate the generation of framework vacancies upon various treatments. The fingerprint region, the range of framework vibration of zeolites (1400-400 cm^{-1}), gives information on the structure. The appearance of bands around 930 cm^{-1} show framework defects [63].

The specific surface area of the zeolites can be measured by volumetric adsorption method using N_2. The adsorption isotherms of zeolites belong to Type I according to the classification proposed by Brunauer, Deming, Deming and Teller (BDDT) [64]. It is generally agreed that if Type I isotherm is obtained for the adsorption on a given solid, then the solid must be predominantly microporous in nature. The zeolites differ from amorphous oxide or active carbon support, since the pore diameters of the zeolite are well determined, while for the other supports it changes in wide range and there is a pore size distribution. The surface area is calculated on the basis of BET equation [65].

The combined thermal analysis (TG, DTG and DTA) gives enlightenment for the quantity of molecules (e.g., water) encapsulated in the zeolite matrix during synthesis.

To characterize the acidity of solid samples the following points have to be considered: (i) the nature (Lewis or Brønsted) (ii) the concentration and (iii) the strength of acid sites.

Infrared spectroscopic methods can supply full-scale information. Using weak bases such as pyridine or ammonia for the adsorption studies the Lewis and Brønsted acidity of the solid can be distinguished, since the pyridinium or ammonium ion and the coordinatively bound pyridine or ammonia have different absorption bands. The concentration of acid centers can be calculated from the integrated absorbances if the corresponding extinction coefficients are known. Finally, the strength of the acidity can be inferred from the shift of the absorption band. The higher the wavenumber of the band is, the higher the strength of acidity is [66].

The acidity of the solid samples can be compared by acid-sensible test reactions as well [33, 67]. For this purpose double bond isomerization of 1-butene can be used. The transformation of 1-butene to cis or trans 2-butene is kinetically first order reaction. It takes place on both acidic and basic centers. The initial reaction rate is in correlation with the number of acidic or basic sites. The initial cis/trans ratio of 2-butenes is different for acidic and basic centers. It is around 1 in the case of acidic and larger than 2 for basic catalysts.

Adsorption of benzene is widely used for characterizing the active centers of the catalysts. Nowadays, chlorobenzene is applied as well, for this purpose. The adsorption of benzene molecules induces changes in the molecular structure, thus, in the molecular symmetry and the vibration spectrum. Barthomeuf et al. [68, 69] studied the location of benzene in a large number of zeolites (in alkaline exchanged X- and Y-faujasite, NaEMT and KL). They investigated the shifts of the C-H out-of-plane bands of benzene molecules adsorbed on the cations or the framework oxygen of the 12 R windows. Gil et al. [70] studied the properties of zeolitic hydroxyl groups in Y- and X-faujasites. The IR spectra of hydroxyls being in interaction with benzene or chlorobenzene molecules show a frequency shift increasing with the acid strength of the center. They proved the presence of hydroxyl groups of different strengths.

The shift of the hydroxyl vibrations has been studied for HZSM-5 zeolites of different aluminum contents [71]. It was found that either the benzene is not an

appropriate probe molecule to differentiate the acid sites with different strength or the strength does not vary in a function of the aluminum content.

The chemisorption of benzene was studied on different metal surfaces (Pt{111}, Cu{110} etc. [72, 73]), and supported metal catalysts (Pt/Al_2O_3 [74, 75, 76, 77], and Ni/SiO_2, Cu/SiO_2 [78]) by IR, near edge X-ray absorption fine structure and high-resolution electron energy loss spectroscopies. It has been found that on the metal surfaces benzene has altering long and short C-C bonds, and it looses the resonance energy by the bonding.

2.3. Decomposition of chlorinated compounds

Halogenated organic compounds are considered to be harmful environmental pollutants. Examples include chlorinated and brominated halocarbons that are environmentally hazardous chemicals, which threaten human health and other biological systems; and chloroflourocarbons (CFCs) that are known to destroy ozone in the stratosphere. These halogenated hydrocarbons are, therefore, receiving much attention for phasing out from industrial sources since emissions are being regulated.

2.3.1. Decomposition of chloroflourocarbons

Chloroflourocarbons (CFCs) have been used for over 40 years because of their beneficial chemical properties and safety to humans. A three-number code is used for exact identification of these compounds. The first number means the number of carbon atoms minus one, the second is the number of hydrogen atoms plus one, and the third is equal to the number of fluorine atoms. If there is one carbon atom in the compound the first number would be zero which is generally not indicated. (For instance: CCl_2F_2 is CFC-12 instead of CFC-012.)

Ozone layer destruction by CFCs was first proposed by Rowland and Molina in 1974 [79]. UV irradiation of CFCs located in the stratosphere generates chlorine atoms, and then the chlorine radicals thus formed decompose ozone molecules to oxygen molecules. Furthermore, CFCs has significantly large greenhouse effect thus used CFCs must be decomposed before entering the atmosphere in order to protect the global environment. However, the several millions of metric tons of CFCs produced so far are still being utilized in the form of refrigerants, solvents and cleaning agents in the electronic industry. Public concern about ozone depletion since the 1980s has led world governments to phase out all CFCs by 1996 in line with the "Montreal Protocol".

Many methods for the destruction of CFCs have been proposed. These methods include incineration, treatments with induced plasma, cement klin, supercritical water or chemical reagents, irradiation by UV-, γ-ray, or ultrasonic

radiation, and catalysis [80]. Among these methods, decomposition using incineration, the cement klin method, and catalysts are thought to be the most useful as far as mass treatment is concerned. However, the incineration method has the disadvantage of producing dioxin as a by-product. The cement klin method is not always useful in mass treatment because the cement produced tends to corrode any reinforcing steel due to its relatively high concentration of chlorine. The catalytic method seems to be the most suitable process for CFC decomposition, because it is an economical decomposition method.

There has been a concerted effort to explore catalysts effective in CFC decomposition. Okazaki reported that Al_2O_3 and SiO_2-Al_2O_3, especially with low Si content show high activity for the decomposition of CFCs [81].

CFC-12 (CCl_2F_2) transforms to CO_2, HF and HCl on the surface of TiO_2 in the presence of O_2 [82]. The activity of the catalyst decreases rapidly because it reacts during the formation of haloids and oxyhaloids. In the presence of water the degradation of catalysts can be retarded, since HCl and HF as products are less reactive than Cl_2 and F_2, which are formed in the absence of water. Besides, the presence of water increases the number of Brønsted acid sites, which have predominant role during the decomposition reaction.

The fluorinated alumina or AlF_3 catalysts are very effective in Cl-F exchange reactions of CFCs [83]. The co-precipitation of magnesium and chromium ions during catalyst preparation lengthens significantly the lifetime of the active catalyst. It was found that Cr^{3+} and Mg^{2+} ions modify the lattice of alumina, the intercalation of Cr^{3+} increases the strength of Brønsted acid sites through the enhanced polarization effect of Cr^{3+}, while Mg^{2+} ions cause the formation of framework vacancies, thus, the Lewis acid centers. Both act as active sites for the catalytic reaction.

Platinum group metals are known to have high hydrogenolytic activity during reforming reactions, therefore, platinum, rhenium, iridium, palladium and ruthenium were selected as active metals for the studies by Bickle et al. [84]. Alumina was selected as support, since upon chlorination alumina is known to have acidic nature and can promote cracking. Pt/Al_2O_3 catalyst had superior performance for CFC-113 destruction compared to Fe/Al_2O_3 at 500 °C over a five-hour trial period. Deactivation rate was, however, too fast for use in a practical

industrial reactor. Deactivation was shown to be due to fluorination of Al_2O_3 by fluorine species produced during the reaction, converting the support to AlF_3. Trials with other platinum group metal indicated ruthenium- and iridium-based catalysts had comparable activities to Pt/Al_2O_3. Palladium- and rhenium-based catalysts were unsuitable because they react with the product chlorine and fluorine species and are lost from the catalyst.

Zeolites are widely examined as potential candidates for CFC decomposition reactions. The research group of our department (the Department of Applied and Environmental Chemistry) has joined to this field some years ago; as a result many publications have been born [85, 86, 87]. The adsorption and decomposition of chlorinated C_1 hydrocarbons (CH_3Cl, CH_2Cl_2 and CCl_4) and chloro-fluorocarbons (CFC-10, –11, -12, and HCFC-22) were investigated on ion-exchanged Y-FAU zeolites by IR and Nuclear Magnetic Resonance (NMR) spectroscopies.

The decomposition of CFCs and chlorinated hydrocarbons takes place *via* the formation of phosgene as intermediate product on samples possessing Brønsted acidity. When the structure of the reactant does not allow the generation of the adsorbed phosgene surface intermediate, it was not detected in the gas phase either. This is the case for $CHClF_2$ and for CH_3Cl. A basic material (Na/NaY-FAU) proved to be inactive in the decomposition reaction. The first step of the mechanism is the adsorption of the molecules on Brønsted acid sites. The conversion in the decomposition of CH_2Cl_2, CCl_4 and CFCs is 100 % above 673 K, but the Y-FAU zeolite is deactivated very quickly, because of the collapse of the zeolite framework. The addition of oxygen to reagents retarded but did not prevent the deactivation of the zeolite.

Two important points have been raised by the ongoing research of the decomposition reaction. One is to clarify the role of acidity in the mechanism. Probably, the molecules interact with the Brønsted acid sites, as can be shown by the shift of the vibrational frequencies of the OH groups, and these sites can supply hydrogen for HCl or HF formation. The other is to improve the resistance of the catalysts to strong acids or reactive intermediate such as phosgene. Prolonged catalyst lifetime is very important for actual application, because it affects the running costs of the reaction system.

Nowadays, beside total decomposition it is particularly promising to convert recovered CFCs catalytically to harmless and preferably useful chemicals. Hydrofluorocarbons (HFCs) are much less harmful to the environment and have some of the useful properties of CFCs and may thus serve as replacement for CFCs. One of the routes to produce HFCs is the reaction between CFC and H_2 catalyzed by noble metals. This reaction may also be used to transform the large amounts of CFCs that exist today into environmentally more benign HFCs.

Palladium is the most extensively investigated catalyst for the hydrodechlorination reaction. Coq et al. [88] thoroughly studied the reaction kinetics of CCl_2F_2 (CFC-12) hydrodechlorination by palladium supported on different carriers: graphite, alumina, AlF_3, ZrO_2 and TiO_2. They established, among various things, that increasing the Pd particle size from 1.5 to 8 nm in a Pd/γ-Al_2O_3 catalyst results in higher hydrodechlorination activity. However, this particle size effect seems to be overshadowed by the influence of the support. At the initial stage of the reaction, Pd/AlF_3 appears much more selective towards CH_2F_2 (a desired product compared to CH_4) than Pd/Al_2O_3; however, after a prolonged reaction time, the latter catalyst acquires a similar performance as Pd/AlF_3. Such a result was interpreted by Coq et al. [88] that hydrodehalogenation induced important changes in Pd/Al_2O_3. The main change observed by XRD was the disappearance of the reflections characteristic of alumina and the appearance of those of AlF_3. Very probably, this transformation occurred by means of the released hydrogen fluoride.

Juszczyk et al. further investigated the role of Pd particle size in the hydrodechlorination reaction of CFC-12 on Pd/ Al_2O_3 catalyst [89]. They concluded that the larger Pd particles are the more easily they are transformed into Pd carbide and the more active and selective they are towards HFC-32 formation. These findings were supported by the results of Ahn et al. [90], namely, the formation of Pd carbide was observed by XPS and XRD during the pretreatment of the catalyst with CHF_2Cl (HCFC-22), which significantly improves the catalytic activity and the catalyst lifetime. Pd carbide is thought to enhance the selectivity towards CH_2F_2 and to prevent sintering of Pd.

Bonarowska et al. examined the role of Au in Pd-Au alloy in hydrodechlorination reaction of CFC-12 [91]. A moderate selectivity for CH_2F_2

exhibited by monometallic Pd/SiO_2 (~40%) is significantly increased up to ~95% with Au addition. Proper Pd-Au alloying is essential to obtain such a selectivity enhancement. Poorly mixed $Pd\text{-}Au/SiO_2$ catalysts show similar behavior as Pd/SiO_2 itself. XRD results indicate the incorporation of carbon in Pd-Au alloy. Gold is sufficient to increase the selectivity for CH_2F_2. Mixed Pd-Au ensembles apparently less strongly adsorb CF_2, thus, give rise to enhanced selectivity towards CH_2F_2.

The hydrogenolysis of CCl_2F_2 over 1 wt.% palladium, platinum, rhodium, iridium and rhenium on activated carbon were studied by Makkee el al. [92]. The main products of the reaction for all investigated catalysts were $CHClF_2$, CH_2F_2 and methane. The generally observed selectivity sequences were Pd << Rh < Pt <Ir << Ru for $CHClF_2$ and Pd >> Pt > Rh >> Ir > Ru for CH_2F_2. From this follows that palladium appears to be good catalyst for the selective conversion of waste CFC-12 into HFC-32. The stability appears to be a function of hydrogen to CFC ratio (an optimal ratio was found at 12) and of temperature (an optimum was found at 510 K). It was shown that the activated carbon support has to be purified prior to the introduction of the Pd, because small amounts of impurities, like Al, Fe or Cr can have significant effects on the catalyst performance. These impurities act as Friedel-Crafts catalyst, thus catalyzing the unwanted chlorine-fluorine exchange.

In the literature the application of hydrodechlorination reaction for other CFCs can be found as well, but these are not as thoroughly reviewed as it is for CFC-12. CCl_3F is commonly used CFC in the manufacture of polyurethane foams, corresponding to nearly 45 % of the total amount of CFCs, but not many alternatives are reported for the treatment of this compound. Ordonez et al. studied the hydrogenolysis of CCl_3F on activated carbon supported noble metal catalysts [93]. The main products of the reaction were methyl fluoride, which is a commonly used compound as cleaning agent in the electronic industries and the manufacture of fine chemicals. Dichlorofluoromethane have similar physical properties as those of CCl_3F, thus, could be a short-term replacement of that compound. Platinum and palladium exhibit high selectivity for CH_3F, whereas ruthenium and iridium are more selective for $CHCl_2F$. Rhodium catalyst exhibits an intermediate behavior with high selectivities for methane. They found that the adsorption of chlorine on the surface plays an important role in product

distribution. Strong chlorine adsorption leads to an increase in the selectivity for $CHCl_2F$. For the time period tested, there were no important deactivation effects, except in the case of iridium.

1,1,2-trichlorotrifluoroethane (CFC-113) may be catalytically transformed to chlorotrifluoroethene (3FCl) or trifluoroethene (3FH) *via* hydrodechlorination without loss of fluorine atoms in the molecule [94]. Both products are monomers for Teflon-like polymers. Furthermore, 3FH can serve as key intermediate in the synthesis of 1,1,1,2-tetrafluoroethane (HFC-134a), a proposed replacement for dichlorodifluoromethane (CFC-12) as a coolant, medical aerosol or foam-blowing agent. More than 80% selectivity in the hydrodechlorination reaction of CFC-113 has been observed over palladium catalysts containing selected metal additives such as Ag, Bi, Cd, Cu, Hg, In, Pb, Sn, Tl to chlorofluoroethene (3FCl) and trifluoroethene (3FH). In particular, bismuth or thallium modified palladium catalyst supported on SiO_2 provided 3FH and 3FCl with more than 90% yield at 520-600 K.

As summary, it can be stated that a possible way of CFC phase out would be their selective conversion to the less harmful HFCs on supported noble metal catalyst. Since the strength of C-Cl bond is lower than C-F bond, the hydrogenolysis of C-Cl can be performed without the cleavage of C-F bond. Although, van de Sandt et al. have established the basis of industrial process for CFC-12 hydrodechlorination [92, 95], the treatment of other CFCs is not solved and is a subject for further investigations.

2.3.2. Decomposition of chlorinated aromatic compounds

Catalytic hydrodechlorination (HDC) appears to be more suitable than incineration for treating chlorinated organic substances, particularly chlorinated aromatic compounds, for which only severe incineration conditions can prevent the formation of polychlorinated dibenzodioxins (PCDDs) or polychlorinated dibenzofurans (PCDFs) at high temperatures. However, they cannot prevent the recombination to dioxins and furans again, once the temperature of the fumes emitted is lowered.

The catalytic hydrodechlorination of aromatic chloro compounds using noble metal based catalysts has been reported [96-111]. Creyghton et al. have

examined Pt/H-BEA and Pt/Al_2O_3 as a catalyst in the HDC reaction of chlorobenzene in the vapor phase at moderate temperature [96]. Both catalysts show high activity in hydrogenolysis of the carbon-halogen bond. Deactivation of Pt/H-BEA is ascribed to acid catalyzed oligomerization reactions and coke formation. This is supported by quantitative differential scanning calorimetry (DSC) and by extraction GC-MS experiments. Replacement of Brønsted acid sites in Pt/H-BEA by sodium ions results in diminished coke formation and improved stability.

The gas-phase catalytic conversion of chlorobenzene has been investigated over Rh/Al_2O_3 and Rh/SiO_2 with metal dispersions varying from 7 to 80 % by Coq et al. [97]. The rates of hydrogenation to chlorocyclohexane and hydrodechlorination to benzene decrease when the dispersion of Rh increases. The influence of the support is negligible on the activity for hydrogenolysis, but noticeable on the activity for hydrogenation.

The kinetics of hydrodechlorination of chlorobenzene has been studied over Pd/Al_2O_3 and Rh/Al_2O_3 catalysts of various dispersions [98]. A reaction scheme is proposed, which is formally analogous to the Mars-van Krevelen mechanism for the oxidation of hydrocarbons. Chlorobenzene interacts with the surface to form a surface chloride and benzene; hydrogen restores a H-covered surface and HCl competes with the reactant for the dechlorination site. The kinetic equation fits well to the experimental data and the rate constants of these three different steps may then be obtained. Influence of particle size appears on the different steps, and particularly on the toxicity of chlorine, which decreases with the size of the metallic particle. The lower reactivity of rhodium catalysts is attributed to more extensive blocking of the surface by chlorine. On Rh/Al_2O_3 the selectivity of benzene or chlorocyclohexane depends on the dispersion of the metal. The formation of chlorocyclohexane is also closely related to the surface coverage in hydrogen under the conditions of reaction. Benzene produced by the main reaction can be hydrogenated to cyclohexane. Compared with the reaction of pure benzene, this reaction shows promoter effect of chlorine in the case of palladium catalysts and inhibition effect in the case of rhodium. This effect can be explained by the known modifications of the metal by the adsorbed chlorine species.

The main problem associated with this reaction on monometallic noble metal catalysts was deactivation due to poisoning by HCl, which is produced during the reaction. Recently, much attention has been focused on bimetallic catalysts to achieve longer lifetime (maintaining higher activity) and higher product selectivity compared to that of monometallic catalysts.

Bodnariuk et al. have reported hydrodechlorination of chlorobenzene in the vapor phase over Pd-Rh/Al_2O_3 and Pd-Sn/Al_2O_3 [99]. On Pd-Rh and Pd-Sn bimetallic catalysts, marked decrease of C-Cl hydrogenolysis is observed, the factor being 10^2-10^3 upon rhodium addition, and larger than 10^6 when tin is added. This behavior is interpreted as follows: on one hand palladium surface atoms are diluted by the second metal; this geometric effect is enhanced by a surface enrichment of the modifier. The driving force for this segregation being the higher affinity of rhodium and tin for the chlorine produced in the reaction. Secondly, there is an electronic interaction between palladium and rhodium or tin, which decrease the reducibility of the chlorine covered palladium surface by hydrogen. This modification is small in the case of rhodium but it is notable when tin is added to palladium.

Srinivas et al. have studied the selective vapor-phase hydrodechlorination of chlorobenzene over alumina supported Pt-Mo/Al_2O_3, Pt-V/Al_2O_3 and Pt-W/Al_2O_3 catalysts [100]. It was concluded that the addition of metal oxide (MO_x, M = V, Mo or W) to Pt improves its stability during the hydrodechlorination reaction. Pt-V/Al_2O_3 seems to be more promising catalyst for obtaining cyclohexane. The study clearly demonstrates that by changing the second metallic element (V, Mo or W), it is possible to change the properties of monometallic Pt sites and achieve the required product selectivity.

Systems containing nickel are known to be active catalysts in some hydrogenation reactions [101] and they are useful for hydrodechlorination processes [102, 103]. Ni/γ-Al_2O_3 [103], Ni/SiO_2 [104] and Ni/C [105] showed catalytic activity in the gas-phase hydrodechlorination reaction of chlorobenzene. Ni based catalysts possessing better resistance to deactivation than noble metal loaded ones, but they work at higher temperatures and pressures.

Recently, Cesteros and his co-workers dehalogenated a number of polychlorinated benzene in the gas phase over Ni/Al_2O_3 catalysts [106]. They

concluded that the activity of the different alumina supported nickel catalysts could be related to the hydrogen available at the reaction temperature. However, the selectivity towards benzene could be explained in terms of the hydrogen desorbed at lower temperature, which competes with the aromatic compounds to be adsorbed on the surface of the catalyst. Among the different alumina supports α-Al_2O_3 was proved to be the best carrier for Ni, this catalyst gave the highest selectivity towards benzene, while it was not the most active one. The catalyst developed contained several nickel atoms supported on high-area nickel-spinel ($NiAl_2O_4$). It was prepared by impregnation followed by calcination and reduction [107]. The most active catalyst yields 87 % benzene at 523 K for a conversion of 82 %.

Gioia and Murena have investigated the simultaneous hydroprocessing of chlorine-, nitrogen- and sulfur-containing aromatics, since generally, the organic wastes contain three different type of compounds together [108, 109, 110]. They studied the hydroprocessing of chlorobenzene, benzothiophene and quinoline on Ni-Mo/γ-Al_2O_3 in the presence of hydrogen. The experimental results show that both hydrodechlorination and hydrodesulphurisation (HDS) processes were strongly inhibited by the presence of quinoline. On the contrary hydrodenitrogenation (HDN) reaction was not significantly influenced by the presence of either chlorobenzene or benzothiophene. The reason for this behavior resides in the fact that the nitrogen containing compounds are strongly basic and adsorb preferentially on the acidic catalyst surface.

We can mention as curiosity, that Couté et al. have reported a novel method for the dechlorination of chlorocarbons by steam reforming [111]. As an alternative approach, steam reforming has several advantages:

(i) Using steam instead of H_2 is safer in industrial processes;

(ii) Complete conversion can be achieved at high space velocities;

(iii) Useful products such as CO, H_2 and non-chlorinated aromatics can be obtained.

Ni/Al_2O_3 and Pt/Al_2O_3 were chosen for catalytic tests. Research have demonstrated that steam reforming with Ni and Pt catalysts is effective for the dechlorination of chloroaromatic compounds, although the activity of Pt is an order of magnitude greater than that of Ni. There is a significant parallel reaction, in

which hydrogen produced by steam reforming removes chlorine through hydrogenolysis, without destroying the ring. Platinum is more selective towards hydrogenolysis than Ni. Significant pyrolysis reactions are present when unreacted chlorocarbons are present. These reactions lead to coke formation that quickly deactivates the catalyst. For practical applications, process conditions must be optimized to ensure high conversion.

3. AIMS

The catalytic treatment of environmentally hazardous chlorinated hydrocarbons, as can be seen from the part where the literature results were reviewed, is the scope of many fundamental researches. In the treated literature there were no references for the application of mono- or bimetallic ZSM-5 type zeolite catalysts in the decomposition reaction of chlorinated compounds. However, we reckon that well-dispersed metal particles in this matrix would be suitable catalyst for this type of reactions.

We have found that the investigation of bimetallic particles in ZSM-5 zeolite host is not so common as it is for Y-FAU zeolites. The question arises: is ZSM-5, which has high Si/Al ratio, an applicable host for bimetallic alloy formation, or are the exchanged metal ions too far from each other not to obtain bimetallic particles during the reduction?

The studies of bimetallic catalysts seem to have holes since the role of Brønsted acidity, which is generated during the reduction by hydrogen, is not sufficiently clarified in the mechanism of different catalytic reactions. We have not found works, which show the characteristics and performance of zeolite catalysts with the same metal loading but different acidity.

The following aims were appointed to clarify the questions and insufficiencies arisen:

- to incorporate one- or two metals, namely copper cobalt or platinum ions and copper-platinum or cobalt-platinum ion pairs into ZSM-5 type zeolite by ion-exchange, and reduce them to get metallic phase using different reduction methods,
- to examine the changes in the structure due to the different treatments by various techniques (XPS, XRD, FT-IR, TG-DTG, ^{23}Na-NMR and volumetric adsorption methods),
- to study the effect of different reduction methods on the Brønsted and Lewis acidities of the catalysts by pyridine adsorption and acid sensitive test reaction,

- to show the presence of bimetallic particle (metallic character, metallic adsorption centers) by benzene or chlorobenzene adsorption methods,
- to investigate the performance of catalysts prepared in C-Cl decomposition reactions (i) for chlorobenzene as model compound of aromatic chloro-compounds and (ii) for carbon tetrachloride as model compound of CFCs.

4. EXPERIMENTAL METHODS

4.1. Preparation of the catalysts

Three different portions of mono- and bimetallic catalysts in ZSM-5 matrix were prepared. The first portion (A) was used for detailed characterization (for checking surface concentration, crystallinity, surface area, and changes in acidity). The second one (B) was applied for CCl_4 decomposition reactions, and the third one (C) was utilized in benzene and chlorobenzene adsorption experiments and in hydrodechlorination reaction of chlorobenzene.

(A) The first portion of catalysts were prepared by ion-exchange of NaZSM-5 zeolite (nominal modulus: Si/Al=40) in a solution of 0.1 M $CoCl_2 \cdot 6H_2O$ (c.p. *Reanal*) $CuCl_2 \cdot 6H_2O$ (c.p. *Reanal*) or $[Pt(NH_3)_4]Cl_2 \cdot H_2O$ (c.p. *Aldrich*), while stirring for 24 h at 333 K to prepare the corresponding Co- Cu- and PtZSM-5 samples. The samples were washed chlorine-free and dried at 373 K. Having determined the degree of ion-exchange, an equivalent amount of $[Pt(NH_3)_4]Cl_2 \cdot H_2O$ complex was dissolved in water and the solution of the complex was added dropwise to the suspension containing either CoZSM-5 or CuZSM-5 under stirring. After 24 h the samples were filtered, washed and dried at 373 K.

(B) At the second portion of samples Na,HZSM-5 (received from MOL RT, nominal modulus: Si/Al= 40) was the parent sample. CoZSM-5 were prepared by ion-exchange in a solution of $Co(NO_3)_2 \cdot 6H_2O$ (c.p. Reanal) as described in section (A). For preparing PtZSM-5 and the two-ionic Pt,CoZSM-5 sample an equivalent amount of $[Pt(NH_3)_4](NO_3)_2$ (c.p. Aldrich) was dissolved in distilled water. While stirring, a solution containing the $[Pt(NH_3)_4]^{2+}$ ion was added dropwise to the Na,HZSM-5 or CoZSM-5 solid containing suspensions. After 24 h stirring the solution was evaporated.

(C) The third portion of catalyst were prepared similarly to method (A). The parent sample was NaZSM-5 (nominal modulus: Si/Al=40). The only difference was that 0.1 M solution of $Co(NO_3)_2 \cdot 6H_2O$, $Cu(NO_3)_2 \cdot H_2O$(c.p. Reanal), and $[Pt(NH_3)_4](NO_3)_2$ were used for the ion-exchange.

Before reduction the samples were pretreated in air flow in order to decompose the $[Pt(NH_3)_4]^{2+}$ complex ion. The samples were heated up to 673 K in a flow of air (50 cm^3/min), at a rate of 1 K/min and kept at that temperature for 10 h.

Each Pt containing sample was divided into two parts before reduction. The first portion of the samples was suspended in distilled water and 250 cm^3 of 0.1 M aqueous $NaBH_4$ (c.p. *Aldrich*) solution was added dropwise. The suspension was stirred for 8 h, filtered and dried. The second portion of the samples was heated up to 573 K in nitrogen flow (50 ml/min) at a rate of 1 K/min, then the gas stream was switched to hydrogen (50 ml/min) and maintained under hydrogen for 7 h.

4.2. Characterization of the catalysts

4.2.1. Composition of the samples

The composition of the parent samples was determined by classical analytical methods. After basic decomposition SiO_2 was filtered weighed and fumed off by HF treatment. The aluminum content was titrated from the mother liquor by complexometry.

The degree of ion-exchange for CoZSM-5 and CuZSM-5 was determined by complexometric titration from the filtered ion-exchange solution.

All the separated solids were analyzed by X-ray fluorescence spectroscopy (XRF) using home-made standards. The Co-, Cu- and PtZSM-5 standards were prepared by impregnation of a given amount of Co, Cu and Pt ion onto the parent zeolites.

^{23}Na MAS-NMR spectroscopy (BRUKER 400 MHz equipment) was applied to determine the concentration and coordination of sodium ions at 105.8 MHz and 1.0 μs ($\Theta=\pi/12$) pulse was used with repetition time of 0.1 s. The spectra were recorded in cooperation with the group of Dr. János B.Nagy (at Laboratoire de RMN, Facultes Universitaires Notre-Dame de la Paix, Namur, Belgium).

The surface concentration and the oxidation state of the various metals were studied by X-ray Photoelectron Spectroscopy in cooperation with Dr. Zoltán Schay (at Department of Surface Chemistry Research Center, Hungarian Academy of Sciences). XPS spectra were measured by a Kratos XSAM-800 cpi ESCA equipment using Al K_α X-ray source for excitation.

4.2.2. Crystallinity and structure

Crystallinity of the zeolites was checked by XRD using DRON-3 X-ray diffractometer. Powdered solids were measured in a range of 2θ = 3° - 43°. For X-ray source the $K_{\alpha 1}$ line of copper anticathode was selected by monocromator. The intensities of the reflections were compared to characterize the degree of crystallization of the catalysts after various treatments.

Infrared spectroscopy (KBr technique) was used to check the generation of framework vacancies upon various treatments. 1 mg of sample was diluted in 200 mg KBr (for IR spectroscopy *c.p. Aldrich*) matrix. The spectra were recorded by a Mattson Genesis spectrometer. Resolution was 1 cm^{-1}. 16 scans were accumulated for a spectrum.

Volumetric adsorption apparatus was used to determine the specific surface areas of the specimens. Adsorption isotherms were obtained at the temperature of liquid N_2 (77 K). For calibrating the dead volume helium was applied. The catalysts were pretreated at 723 K under continuous evacuation for 1 h. The specific surface area of the sample was calculated from the isotherm by the BET method.

4.2.3. Characterization of the adsorption centers

The adsorption centers of the catalysts were investigated by IR spectroscopy using different probe molecules. The acidity of the samples was determined by pyridine (c.p. *Interkémia*) adsorption technique. Benzene (c.p. *Reanal*) and chlorobenzene (c.p. *Reanal*) were applied to study the behavior of the different metals in the zeolite matrix.

Self-supported wafers (10 mg/cm^2) were prepared from the powdered zeolites and placed into the sample holder of the *in situ* IR cell. Pretreatment of the samples was as follows. The temperature of the wafer was slowly increased to 723 K under continuous evacuation of the cell. After 2 h treatment, the sample was cooled to room temperature and the background spectrum of the zeolite was recorded. The resolution of the spectra was 1 cm^{-1}. 16 scans were accumulated for a spectrum.

(i) For the acidity measurements 1.33 kPa pyridine was introduced into the cell at ambient temperature, which was then heated to 473 K. After 1 h equilibration, the cell was evacuated for 1 h at the same temperature. The sample was cooled down and the spectra of pyridine bonded by the Brønsted and Lewis acid sites were recorded. The absorbances were integrated, the areas were divided by the mass of the wafer and these values were used for the comparison of the acidities.

(ii) For benzene and chlorobenzene adsorption measurements generally 1.33 kPa benzene or chlorobenzene was introduced onto the pretreated wafer at room temperature. After the equilibration the cell was evacuated at room temperature for 2 minutes, and a spectrum was registered. The procedure was repeated after 30 minutes evacuation at room temperature, and at 373 K.

4.3. Catalytic reactions

4.3.1. Double bond isomerization of 1-butene

The acidity of the catalysts was characterized by double bond isomerization of 1-butene (c.p. *Aldrich*) in a circulatory batch reactor. 100 mg of catalyst was placed into the reactor and pretreated at 723 K under continuous evacuation for 1 h. In some cases this was followed by *in situ* hydrogen treatment at 573 K. The reactor was cooled down to the reaction temperature (323 K) followed by introduction of 66.6 kPa 1-butene into the reactor. The reacting gas mixture was analyzed by on-line gas chromatography (GC) (Hewlett Packard 5710 type Gas Chromatograph) equipped with flame ionization detector (FID). The isomers – 1-butene, *cis* and *trans* 2-butene – were separated at 293 K on a 4.5 m column loaded with 30 % dimethyl-sulfolane/Chromosorb W.

4.3.2. Hydrodechlorination of chlorobenzene

Hydrodechlorination reaction of chlorobenzene was performed in (i) an *in situ* IR cell using self-supporting wafer technique and (ii) in tubular reactor made of glass in flow system applying GC product analysis.

(i) The measurements were performed as described in chapter 4.2.3. 1.33 kPa chlorobenzene and 13.3 kPa hydrogen were introduced into the cell and heated up to the reaction temperatures (273 K, 373 K or 473 K). After 0.5 h reaction time the cell was cooled down and the spectra of both the gas phase and adsorbed species were recorded.

(ii) The hydrodechlorination reaction was also studied in a flow reactor system. The catalysts were placed into the reactor and pretreated at 723 K in N_2 then H_2 flow with a flow rate of 25 ml/min. Then, the sample was cooled down to the reaction temperature. 5 ml of chlorobenzene was dosed into the reactor with a rate of 0.05 ml/min, in a constant H_2 stream. The products were collected in ice traps, and analyzed by CHROM-5 GC equipped with FID using polyethylene glycol (Carbowax 1200) as separation phase on Chromosorb W support. The HCl formed during the reaction was passed

through of 1 M NaOH solution, then the chloride ion was titrated by argentometric method.

4.3.3. Transformation of CCl_4 under oxidative, neutral and reductive conditions

Transformation of CCl_4 (c.p. *Reanal*) was carried out in a flow system applying IR spectroscopic product analysis. The catalysts placed in a glass reactor were pretreated in N_2 stream (25 ml/min) at 723 K for 1 h. After adjusting the desired reaction temperature (generally we started the reaction at room temperature) carbon tetrachloride was fed using either nitrogen, oxygen or hydrogen flow with a flow rate of 10 ml/min. The gas stream containing the products formed was passed through an IR gas cell and the spectra were taken at predetermined times (generally after 0.5 h reaction time). The resolution of the spectra was 1 cm^{-1}. 16 scans were accumulated for a spectrum. Then the temperature of the reactor was raised stepwise up to 573 K, while the products were analyzed after each step.

5. RESULTS AND DISCUSSION

5.1. Composition of the zeolite catalysts

5.1.1. Composition of the bulk phase

The compositions and the moduli (Si/Al ratio) of the parent zeolites were determined by classical analytical methods. Data obtained are summarized in Table 1. (A), (B) and (C) means the group of catalysts prepared according to chapter 4.1. These symbols are maintained and used in the whole chapter for identifying the samples used in different experiments.

	Compound	Nominal Modulus	Measured Modulus	Unit cell composition
(A)	NaZSM-5	40	40.0	$Na_{2.4}Al_{2.4}Si_{93.6}O_{192}$
(B)	Na,HZSM-5	40	33.0	$Na_{0.87}H_{2.13}Al_{3.0}Si_{93.0}O_{192}$
(C)	NaZSM-5	40	38.6	$Na_{2.43}Al_{2.43}Si_{93.57}O_{192}$

Table 1. *The nominal and measured modulus and unit cell composition of parent zeolites*

The degree of ion-exchange for the different compounds was determined and supported several ways. Calculated data can be seen in Table 2.

Firstly, the transition metal content of CoZSM-5 (A) and CuZSM-5 (A) or the noble metal loading of PtZSM-5 (A) catalysts was calculated from the sodium content of the prepared samples, which was measured by ^{23}Na NMR spectroscopy. These data were supported by the complexometric titration of the ion-exchange mother liquor for CoZSM-5 (A) and CuZSM-5 (A). Data measured in various ways showed good agreement. The composition of Pt,CoZSM-5 (A) and Pt,CuZSM-5 (A) were determined after XRF analysis of each sample.

The degree of ion-exchange for CoZSM-5 (B) was calculated from the cobalt ion loss of the ion-exchange solution. The platinum content of PtZSM-5 and Pt,CoZSM-5 is exactly the same as the cobalt ion content, since the same amount of tetraamine platinum salt was impregnated onto Na,H- and CoZSM-5 zeolites.

The composition of the third set of catalysts (C) was determined by XRF analysis using home-made standards. The standards were analyzed by classical analytical methods after decomposition. The CoZSM-5 (C) sample was also demineralized and titrated to check the reliability of the standards. The mother liquor after ion-exchange were titrated in the case of Co- and CuZSM-5 (C) catalysts, as well. The data, again, gave good correlation.

	(A)			(B)		(C)		
	Co- %	Cu- %	Pt- %	Co- %	Pt- %	Co- %	Cu- %	Pt- %
CoZSM-5	67			10		71		
CuZSM-5		97					81	
PtZSM-5			93		10			57
Pt,CoZSM-5	46		51	10	10	63		43
Pt,CuZSM-5		45	55				65	49

Table 2. *The degree of ion-exchange for the different catalysts*

The degree of ion-exchange is above 100 % in the case of Pt,Co- and Pt,CuZSM-5 (C). The explanation of this comes from the fact that for zeolites with high modulus during transition metal ion-exchange the heterolytic splitting of coordinatively bound water can occur according to Scheme 1 [112]:

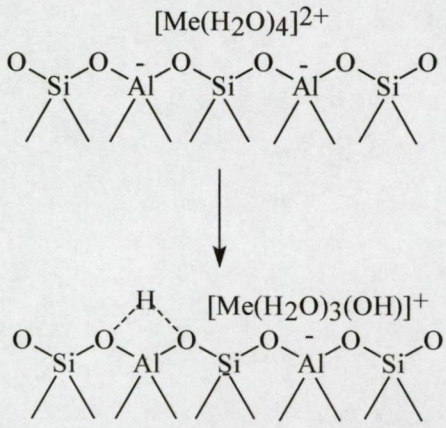

Scheme 1. *Heterolytic splitting of coordinatively bound water of metal cation in zeolite framework*

In the second ion-exchange step the H^+ ion can be exchanged to $[Pt(NH_3)_4]^{2+}$ cation. Thus, the charge of the transition metal complex ion is +1, while the degree of ion-exchange is calculated as if it was two.

5.1.2. Surface concentrations

X-ray photoelectron spectroscopy (XPS) was employed to measure the surface concentration of the various components using the intensities of Cu 2p, Co 2p, Si 2p, and Pt 4f peaks. The surface concentration of Pt, Cu and Co were determined and the Cu/Si, Co/Si and Pt/Si surface atomic ratios indicated the presence of these components in the samples after reduction both by H_2 and $NaBH_4$. Surface concentrations are presented in Table 3 and values are compared with bulk compositions.

Sample	Re-duced with	Co/Si		Cu/Si		Pt/Si		Valence state
		Bulk	Surf.	Bulk	Surf.	Bulk	Surf.	
Pt,CoZSM-5 (A)		0.008				0.008		
	H_2		0.025				0.015	Co^{2+}, Co^0, Pt^0
	$NaBH_4$		0.047				0.008	Co^{2+}, Co^0, Pt^0
Pt,CuZSM-5 (A)				0.012		0.012		
	H_2				0.012		0.012	Cu^0, Pt^0
	$NaBH_4$				0.042		0.037	Cu^0, Pt^0

Table 3. *Surface concentration and valence state of Co, Cu and Pt in Pt,CoZSM-5 (A) and Pt,CuZSM-5 (A) samples calculated from the Co 2p, Si 2p, Cu 2p and Pt 4f ratios measured by XPS*

Pt $4f_{7/2}$, Co $2p_{3/2}$ and Cu $2p_{3/2}$ binding energies were used to determine the oxidation state of the various metals after reduction. The Pt $4f_{7/2}$ binding energy is equal to 314.2 and 314.1 eV after reduction in H_2 and $NaBH_4$, respectively, while the respective Cu $2p_{3/2}$ binding energies are 932.3 and 931.9 eV. These values indicate that regardless of the mode of reduction, both metals have zero oxidation state. On the contrary, in Pt,CoZSM-5 (A) only Pt is reduced by either H_2 or $NaBH_4$, whereas about 90 % of the cobalt ions were not reduced (Figure 2). It is worth mentioning that the surface Co/Si ratio is much higher than the ratio calculated from the chemical composition. It means that part of the Co was spread on the outer surface, probably in the form of oxide.

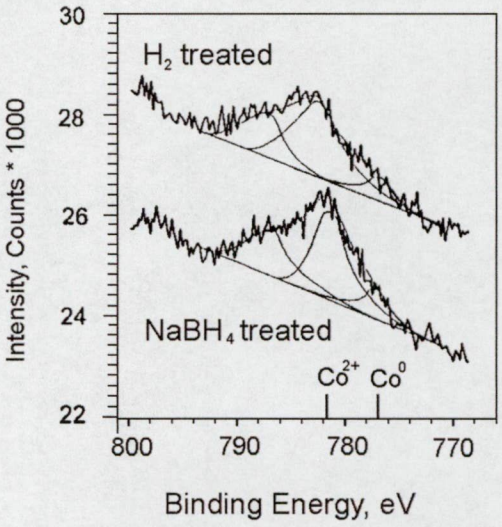

Figure 2. *Co 2p XPS spectra of H_2 and $NaBH_4$ treated Pt,CoZSM-5 (A) catalysts*

5.2. Structure of the catalysts

The crystallinity of the parent samples – NaZSM-5 (A), Na,HZSM-5 (B) and NaZSM-5 (C) – was checked by X-ray diffractometry (XRD) (Figure 3). The XRD spectra showed good agreement with the data of XRD atlas for zeolites [62].

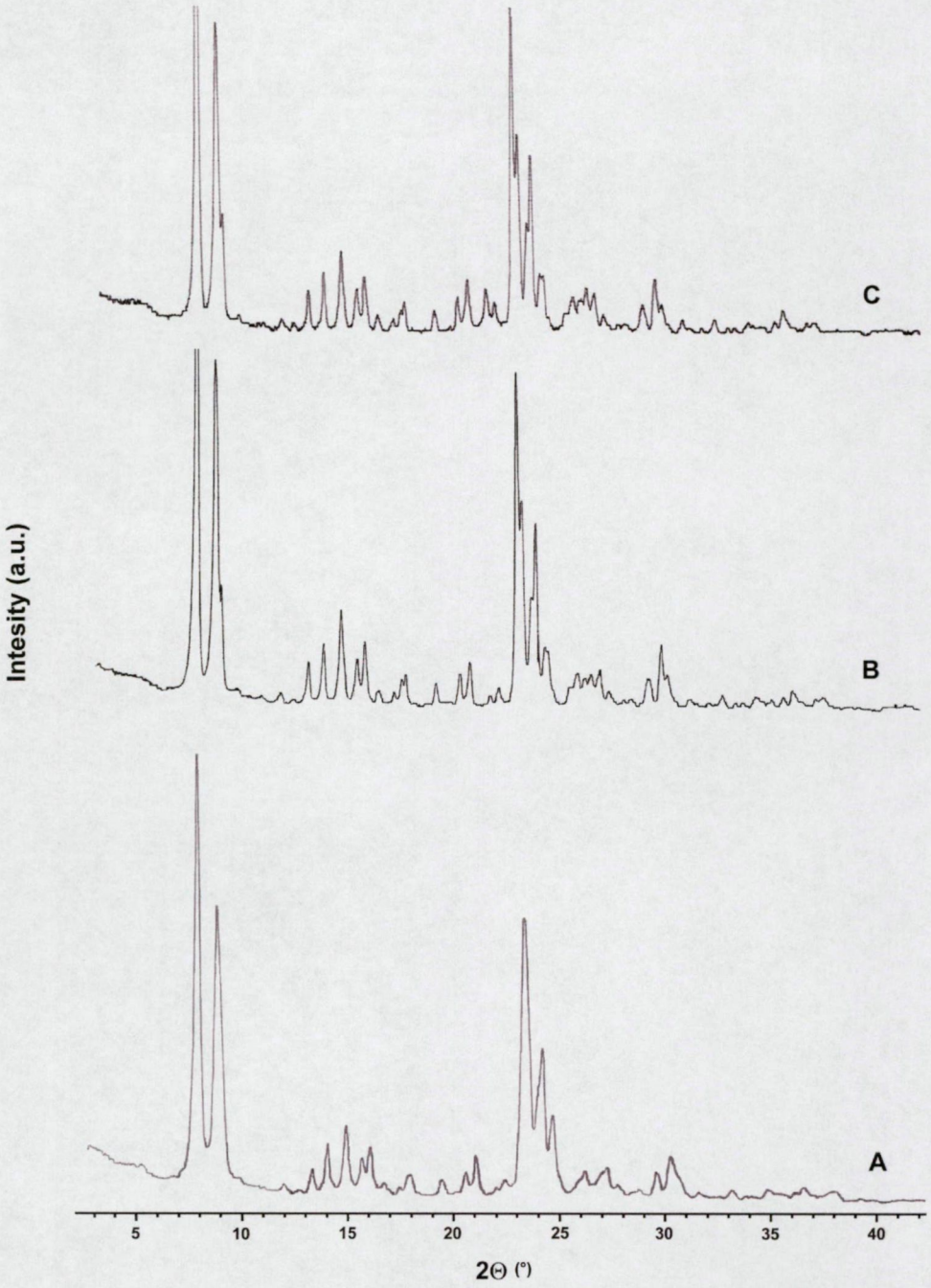

Figure 3. *XRD spectra of parent ZSM-5 zeolites*

The XRD spectra of the platinum containing samples resembled to that of the parent sample to a great extent (see Figure 4), except that a weak Pt reflection at $2\theta = 40°$ could be observed. These weak and broad bands indicate the presence of small platinum metal crystals in the nanoscale range. It was found that the various way of reducing the ion-exchanged ZSM-5 zeolite did not bring about significant changes in its original structure. In contrast with Y-FAU hosted Pt zeolites, where the migrating and aggregating large platinum crystallites push apart portions of the zeolite crystals, the ZSM-5 structure with high modulus is stable enough not to be damaged during these sort of processes.

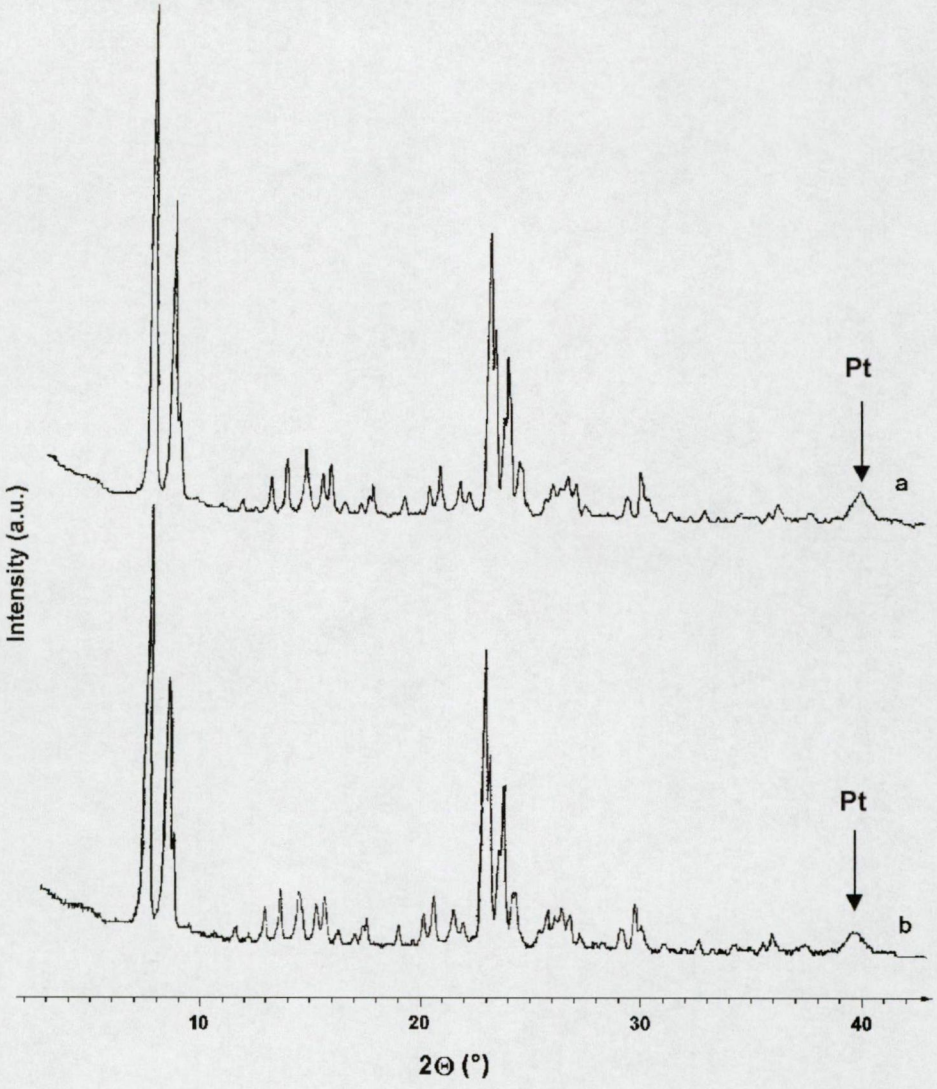

Figure 4. *XRD spectra of PtZSM-5 (C)* ***a:*** *reduced by* H_2 ***b:*** *reduced by* $NaBH_4$

However, there are differences in the intensities of the Pt reflection for the various catalysts as can be seen on Figure 5. They can be attributed to different Pt loadings (Pt- versus Pt,CoZSM-5 (A)), as well as to the different migrating abilities of the metals (Pt,Co- versus Pt,CuZSM-5 (A)). In the case of Pt,CuZSM-5 (A) reduced in H_2 the reflection characteristic for platinum shifts towards higher 2θ values. Presumably, copper, which has a lower lattice constant ($d(Cu)_{100}$ = 209 ppm) value than that of the platinum ($d(Pt)_{100}$ = 227 ppm), intercalated into the platinum crystalline and shifted the reflection towards the higher 2θ value. To detect such a shift in XRD reflection generally the presence of 5 % of modifier atom is needed. Accordingly, the presence of bimetallic Pt-Cu particle is likely in this case.

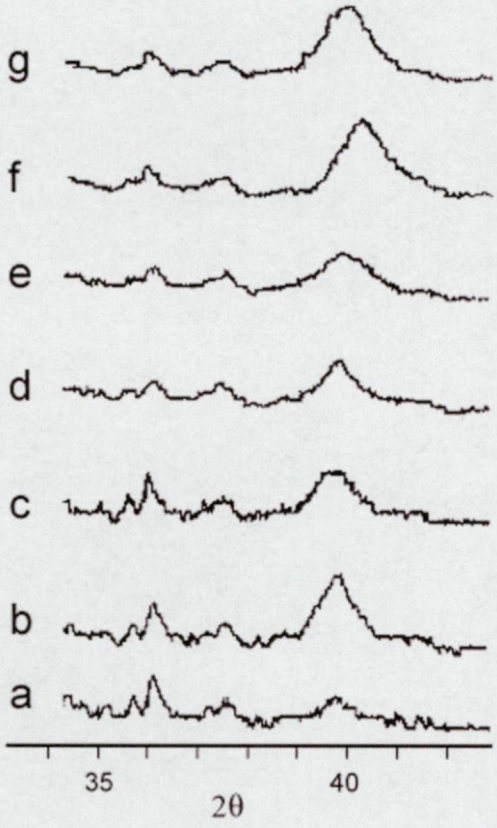

Figure 5. *XRD reflections of*
a: *PtZSM-5 (A) (before red.)*
b: *PtZSM-5 (A) (red. by H2)*
c: *PtZSM-5 (A) (red. by NaBH4)*
d: *Pt,CoZSM-5 (A) (red. by H2)*
e: *Pt,CoZSM-5 (A) (red. by NaBH4)*
f: *Pt,CuZSM-5 (A)(red. by H2)*
g: *Pt,CuZSM-5 (A) (red. by NaBH4)*

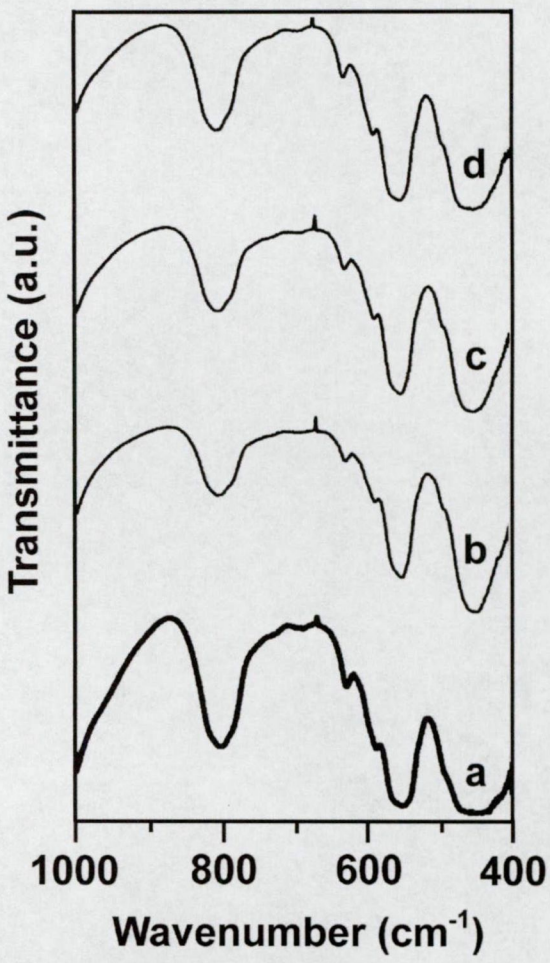

Figrue 6. *IR spectra of catalysts reduced by different way*
a: *Pt,CoZSM-5 (A) red. by H_2*
b: *Pt,CoZSM-5 (A) red. by $NaBH_4$*
c: *Pt,CuZSM-5 (A) red. by H_2*
d: *Pt,CuZSM-5 (A) red. by $NaBH_4$*

IR spectra taken in the range of framework vibration of zeolites (400 cm^{-1} – 1400 cm^{-1}) verify the results of XRD (Figure 6). Spectra in the "finger-print" region did not show any changes after the heat- and reducing-treatment, and no new band appeared at around 930 cm^{-1}, which wavenumber has been assigned to framework defects [63]. Thus the ZSM-5 matrix is a suitable host for well-dispersed noble or transition metal catalyst.

The BET specific surface area of the samples (Table 4) remained very similar independently of the metal exchanged and the method of reduction.

Two types of weight losses can be observed on the thermogravimetric (TG) curve of the samples. Both of them are assigned as water-loss processes. The first step at around 373 K is attributed to the loss of crystal water of the zeolite. The second weight loss, appearing at high temperature, indicates the leaving of water formed by dehydroxylation of the surface hydroxyl groups.

Studying the peculiarities of weight losses between the bimetallic compounds (Table 4) one can conclude that there is difference between the copper- and cobalt-containing catalysts. The Co-containing samples adsorb more water in an atmosphere saturated with water. Since the cobalt ion is not reduced completely – as it is concluded from the results of XPS and IR acidity measurements –, it can take up coordinatively bound water.

Sample	Reduced with	Surface area (BET) m^2/g	Weight loss at 1200 K m%
NaZSM-5 (A)		322	4.90
CoZSM-5 (A)		341	7.17
CuZSM-5 (A)		352	8.55
PtZSM-5 (A)	H_2	302	5.70
	$NaBH_4$	310	5.17
Pt,CoZSM-5 (A)	H_2	328	8.87
	$NaBH_4$	292	8.03
Pt,CuZSM-5 (A)	H_2	331	5.38
	$NaBH_4$	313	5.19

Table 4. *Characteristics of the catalysts*

5.3. Acidity of the catalysts

The Brønsted and Lewis acid centers play significant role in a large number of heterogenous catalytic reactions. To uncover the mechanism of a reaction the accurate knowledge of the acid centers – both the quality and quantity – are indispensable. Furthermore, it may also be an aim to prepare catalysts with identical metal loadings but different acidities.

The acidity of the catalysts, used in our investigations, were studied by infrared spectroscopy, using pyridine as probe and by the reaction of 1-butene double bond isomerisation.

5.3.1. Pyridine adsorption

The IR bands appeared in the region characteristic of both Brønsted and Lewis acid sites at 1545 and 1455-1440 cm^{-1}, respectively. The band generally appearing at 1490 cm^{-1} is attributed to a combination vibration characteristic both Brønsted and Lewis acidities.

Figure 7 shows the spectra of pyridine adsorbed on the monoionic samples. There is only negligible amount of Brønsted acid sites on the NaZSM-5 (A) (spectrum a) sample. The intense band at 1445 cm^{-1} is assigned to pyridine bonded coordinatively to the sodium ions. The spectrum of pyridine adsorbed on CuZSM-5 (A)

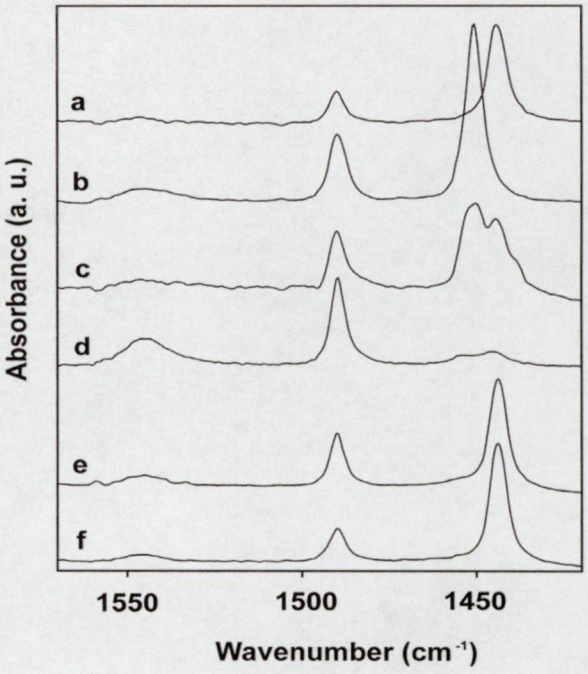

Figure 7. *IR spectra of adsorbed pyridine on* ***a*** *NaZSM-5 (A),* ***b*** *CuZSM-5 (A)* ***c*** *CoZSM-5 (A)* ***d*** *PtZSM-5 (A) reduced in H_2* ***e*** *PtZSM-5 (A) reduced in $NaBH_4$* ***f*** *PtZSM-5 (A) reduced in $NaBH_4$ followed by in situ H_2 treatment*

(spectrum b) reveals very weak Brønsted acidity, which is generated from the splitting of the coordinatively bound water (see Scheme 1). However, the intense band at 1451 cm^{-1} is characteristic of the Lewis centers. It is to be noted that for CuZSM-5 (A) this band appeared at somewhat higher wavenumbers, since copper ion is regarded as stronger Lewis center than the sodium ion.

The spectrum of pyridine on CoZSM-5 (A) zeolite (spectrum c) shows more complex structure. The band assigned to the Brønsted acidity is weak, whereas the spectral range in the Lewis site bonded pyridine seems to be quite complex. The bands at 1451, 1445 and 1438 cm^{-1} can be assigned as pyridine linked to cobalt ions, to sodium ions and to physisorbed pyridine, respectively.

The pyridine spectrum of the PtZSM-5 (A) sample reduced in hydrogen (spectrum d) show an intense band of pyridinium ions at 1545 cm^{-1}. On the samples reduced by $NaBH_4$ (spectrum e) the concentration of Brønsted site bonded pyridine is negligible. Postreduction in hydrogen (spectrum e) reveals no significant formation of Brønsted sites, as the spectra [(e) and (f)] are almost identical. In the PtZSM-5 (A) sample reduced by $NaBH_4$ the intense band at 1445 cm^{-1} is assigned to pyridine linked to sodium ions being characteristic of Lewis acid sites. From the spectrum of the hydrogen-reduced sample only a weak band appears at the same wavenumber. A second, low intensity band was found at 1455 cm^{-1}, which is attributed to pyridine adsorbed on true Lewis acid sites generated upon heat treatment by the release of framework aluminum (Scheme 2) [113]:

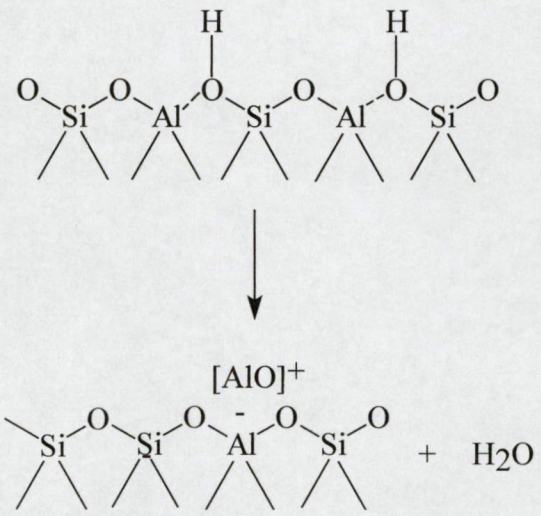

Scheme 2. *Dealumination of zeolites*

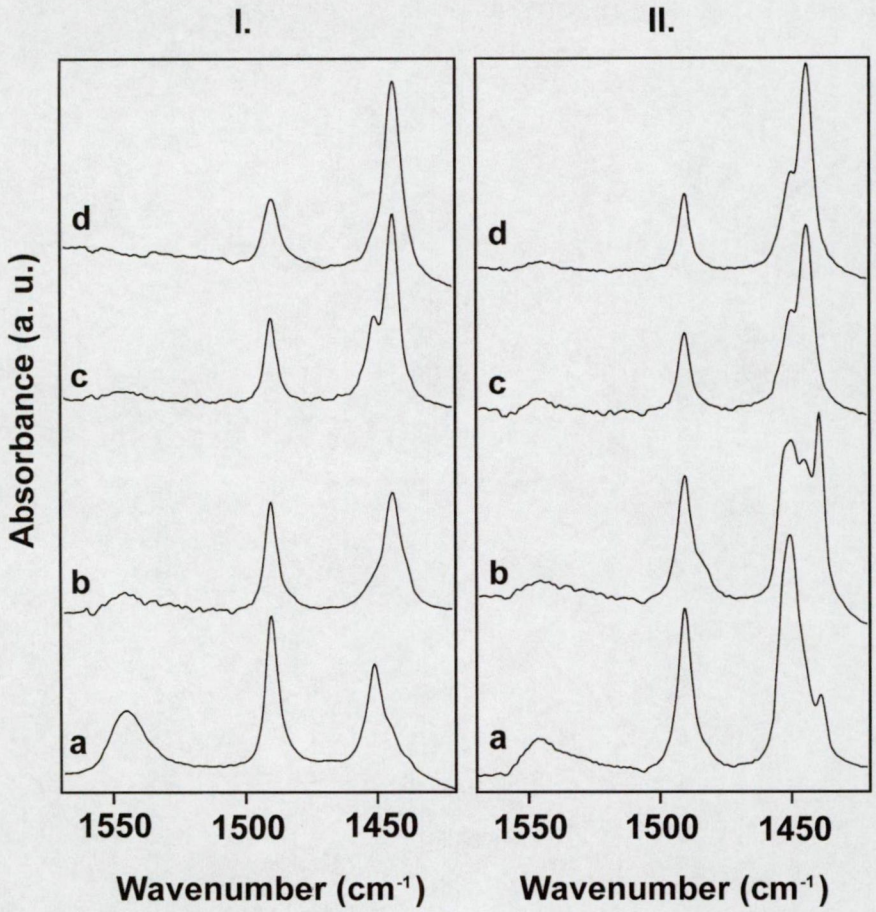

Figure 8. *IR spectra of adsorbed pyridine on* ***I.*** *Pt,CuZSM-5 (A) and* ***II.*** *Pt,CoZSM-5 (A) catalysts reduced in different ways:* ***a*** *by* H_2, ***b*** *by* H_2 *followed by* Na^+ *ion-exchange,* ***c*** *by* $NaBH_4$, ***d*** *by* $NaBH_4$ *followed by in situ* H_2 *treatment*

Figure 8/I. shows the spectra of pyridine adsorbed on Pt,CuZSM-5 (A) samples reduced either by hydrogen (a) or $NaBH_4$ solution (c). As spectrum (a) shows the band characteristic of Brønsted acid sites (band at 1545 cm^{-1}) is prevailing. In the spectral range where pyridine is adsorbed on Lewis acid sites, the most intense band appeared at 1451 cm^{-1}, the low-frequency side of which two shoulders can be seen at 1443 and 1438 cm^{-1}. The band is assigned to pyridine on copper ions, while the shoulder bands are pyridine on sodium ions and physisorbed pyridine, respectively. After Na^+ exchange in NaCl solution (spectrum b), the intensity of the band resulting from Brønsted acid sites substantially decreased and the absorption arising from pyridine bound to sodium ions became predominant. On both sides of this band pyridine on copper ions at 1451 cm^{-1} and a very weak indication of physisorbed pyridine at 1438 cm^{-1} are seen as

shoulders. When the samples were reduced by $NaBH_4$, there is no band originating from the presence of Brønsted acid sites. The secondary reduction with hydrogen did not result in generation of Brønsted acid centers either (see spectrum (d)), although the band intensity of pyridine on copper ions at 1451 cm^{-1} is diminished to a shoulder.

As can be seen in Figure 8/II. the spectra of pyridine adsorbed over Pt,CoZSM-5 (A) zeolites reduced with $NaBH_4$ solution (see spectrum (c)) only traces of Brønsted acid sites are detected. The spectrum taken after hydrogen postreduction (see spectrum (d)) is identical to the parent sample. Pt,CoZSM-5 (A) reduced in hydrogen (see spectrum (a)) contains Brønsted acidity, however, the concentration of these sites gradually decreases upon ion-exchange with NaCl solution.

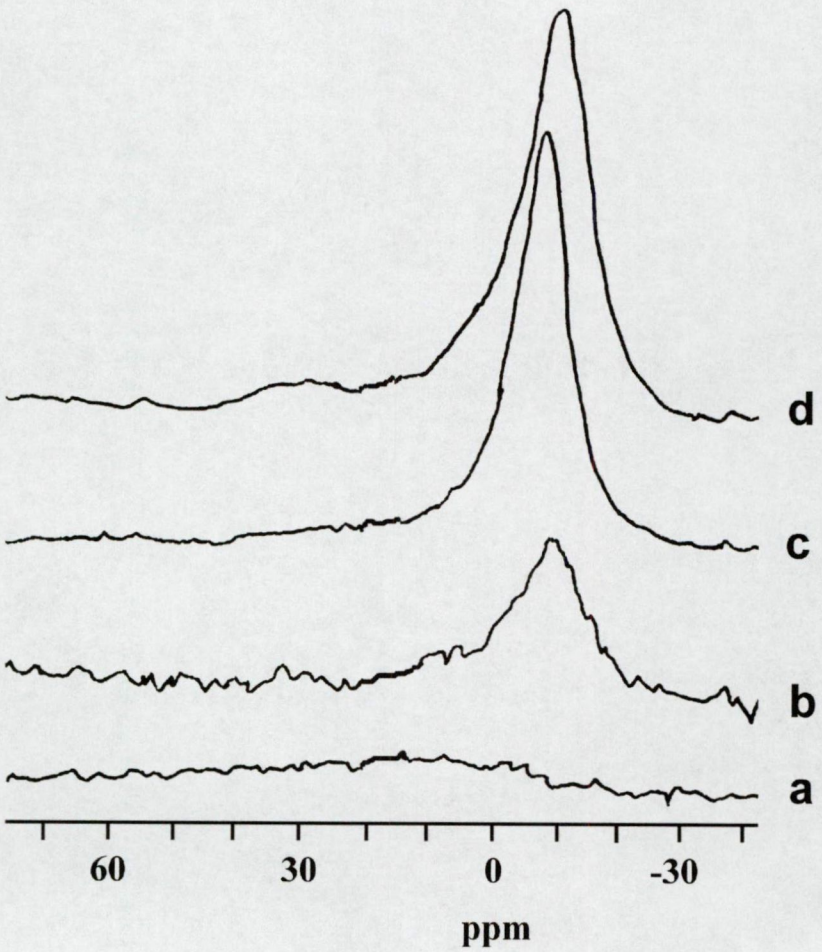

Figure 9. *^{23}Na NMR spectra of bimetallic samples:*
a *Pt,CuZSM-5* ***b*** *Pt,CoZSM-5 reduced by H_2*
c *Pt,CuZSM-5* ***d*** *Pt,CoZSM-5 reduced by $NaBH_4$*

The incorporation of sodium ions can be followed by pyridine adsorption in the spectral range of Lewis sites and can be evidently seen from the ^{23}Na NMR spectra in Figure 9. The sample reduced in hydrogen shows absorption at 1450, 1445 and 1438 cm^{-1} being assigned to pyridine on cobalt ions, sodium ions and physically bound to structural units, respectively. After sodium ion-exchange the intensity of the band due to pyridine on sodium ions and physically bound pyridine increased. In Table 5 the band position and the integrated absorbances are presented.

Sample	Brønsted acid sites		Lewis acid sites			
ZSM-5 (A)	Position (cm^{-1})	A (cm^{-3}/mg)	Position (cm^{-1})			A (cm^{-3}/mg)
Na	n. d.	traces		**1444**	1438	0.34
Cu	1545	0.11	**1451**	n. d.	n. d.	0.54
Co	1547	0.1	**1451**	**1445**	1438	0.62
Pt(H)[a]	**1545**	0.28	1455	1445	n. d.	0.13
Pt(B)[b]	1545	0.06	n. d.	**1443**	n. d.	0.42
Pt(B)(H)[c]	1545	0.05	n. d.	**1443**	n. d.	0.53
Pt,Cu(H)	**1546**	0.18	**1451**	1445	1438	0.16
Pt,Cu(H,Na)[d]	1546	0.11	1451	**1445**	1438	0.42
Pt,Cu(B)	1546	0.05	1451	**1445**	n. d.	0.58
Pt,Cu(B)(H)	1546	traces	1451	**1445**	1438	0.50
Pt,Co(H)	**1546**	0.16	**1450**	1444	1438	0.60
Pt,Co(H,Na)	1545	0.10	**1450**	1444	1438	0.97
Pt,Co(B)	1545	0.07	1450	**1444**	n. d.	0.53
Pt,Co(B)(H)	1545	0.02	1450	**1444**	n. d.	0.51

Table 5. *Band positions of adsorbed pyridine and their integral absorbances divided by the weight of the wafers*

[a](H) means: the sample was reduced in hydrogen.

[b](B) means: the sample was reduced with $NaBH_4$ solution.

[c](B)(H) means: the sample was reduced with $NaBH_4$ solution, then by hydrogen.

[d](H,Na) means: the sample reduced in hydrogen was exchanged in NaCl solution.

Bold figures indicate the dominating bands in the spectrum of adsorbed pyridine; n. d. means that the band was not detected.

5.3.2. Double bond isomerization of 1-butene

The double-bond isomerization of 1-butene can be described by trigonal scheme of reversible, kinetically first order reactions:

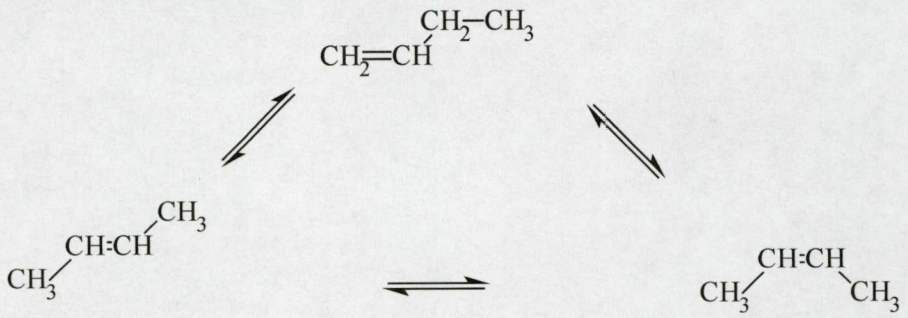

Scheme 3. *Trigonal scheme of 1-butene double bond isomerization*

This test reaction is applicable for characterizing the acidic or basic sites of solid samples. In the initial phase of the reaction the ratio of *cis* and *trans* 2-butene formed is characteristic for the acidity or basicity of catalysts. The difference of cis/trans ratio can be explained by a different transformation mechanism occurring on different sites [67].

In the case of acid catalyzed reaction the transition state of reactant is carbenium-ion and the formation of cis- or trans-2-butene is statistically equal, thus, the cis/trans ratio around 1. On the other hand, the reaction goes through a π-allyl carbanion intermediate bound on basic sites, from which cis-2-butene forms preferentially. In this case the initially measured cis/trans ratio is over 2.

In the current experiments the cis/trans ratio of 2-butenes were around 1 for all of the measured samples, on which the reaction proceeded.

The relative quantity of acid sites can be determined by comparison of the initial reaction rates. The determined reaction rate values for the different catalysts can be found in the figure legends.

As can be seen in Figure 10 the PtZSM-5 (A) sample reduced by H_2 appeared to be very active in the double bond isomerization of 1-butene. The initial reaction rate is commensurable with that of HZSM-5. The sample reduced by $NaBH_4$ is proved to be much less active with reminiscent Brønsted sites characteristic for the zeolite itself. The transition metal loaded zeolite shows

notable activity, as concluded according to the IR measurements, because of the heterolytic dissociation of coordinatively bound water.

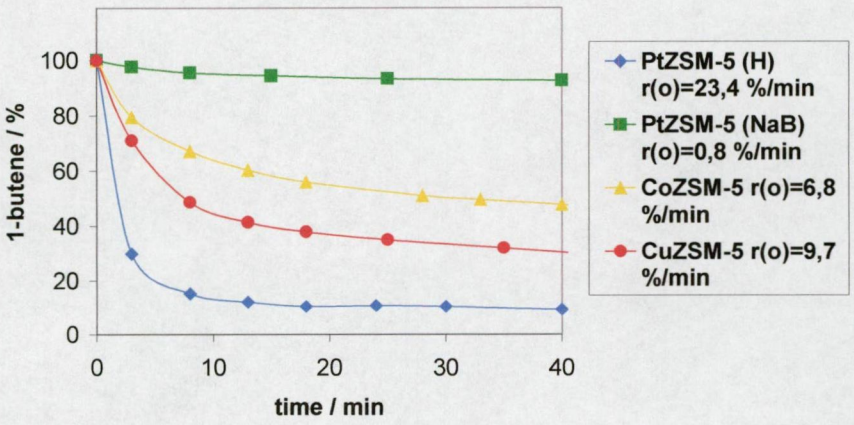

Figure 10. *Kinetic curves of 1-butene transformation over different monometallic catalysts (H) means reduced by H_2 and (NaB) by $NaBH_4$*

Similar conclusion can be drawn for bimetallic zeolites as well (Figure 11 and 12). The hydrogen treated samples (Pt,Cu- and Pt,CoZSM-5(H)) show high activity, while the samples reduced in $NaBH_4$ solution (Pt,Cu- and Pt,CoZSM-5(NaB)) have an initial reaction rate similar to that of the respective transition metal loaded representatives (Cu- or CoZSM-5). When these samples were treated with H_2 at 573 K no further reduction of Pt^{2+}, Cu^{2+} or Co^{2+} took place, since the rate of 1-butene transformation did not change significantly.

We can conclude, that choosing different reduction method results in catalysts with the same metal loading but different acid character. Studying of these catalysts helps in better understanding the role of Brønsted acidity in the mechanism of catalytic reactions.

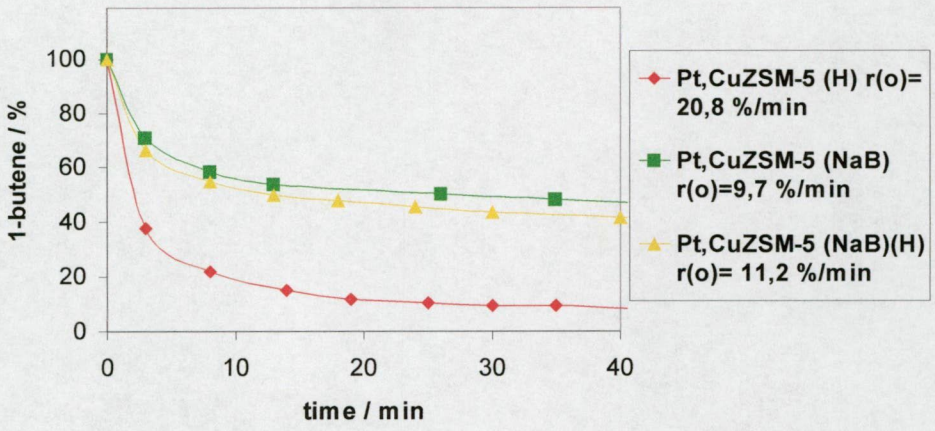

Figure 11. *Kinetic curves of 1-butene transformation over Pt,CuZSM-5 (A) catalysts reduced different way: by H_2 (H), by $NaBH_4$ (NaB) and by $NaBH_4$ followed by in situ H_2 treatment (NaB)(H)*

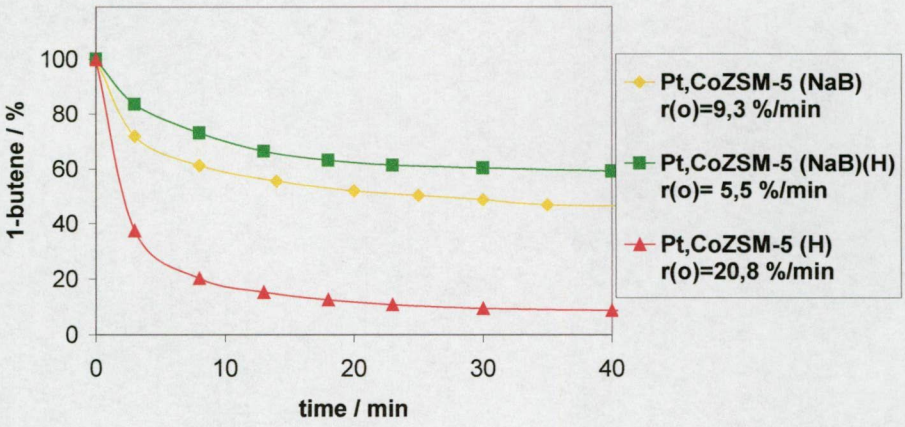

Figure 12. *Kinetic curves of 1-butene transformation over Pt,CoZSM-5 catalysts reduced by different ways: by H_2 (H), by $NaBH_4$ (NaB) and by $NaBH_4$ followed by in situ H_2 treatment (NaB)(H)*

5.4. Adsorption of benzene and chlorobenzene

The shifts of IR vibration bands appearing upon the adsorption of benzene or chlorobenzene refer to various characteristics of the zeolites and various event occurring on them:

(i) The changes in the OH vibration region give information about the acidity of the samples.

(ii) The different shifts of combination vibrations in C-H out of plane region shows whether the molecule adsorbs on the metal cation or the zeolitic framework oxygen.

(iii) The appearance of band characteristic for chemisorbed benzene in C-H stretching region shows the cessation of π-bond delocalization of benzene ring.

In Figure 13 the characteristic IR bands of (i) adsorbed benzene on (a) PtZSM-5 (C) reduced by H_2 (b) CoZSM-5 (C) and (d) CuZSM-5 (C) and (ii) adsorbed chlorobenzene on (c) CoZSM-5 (C) and (e) CuZSM-5 (C) can be seen. Specta were recorded after evacuation of the gas phase benzene or chlorobenzene at room temperature for 2 minutes.

Significant changes could not be detected in vibration of zeolitic OH group upon the adsorption of benzene or chlorobenzene on different catalysts. Probably the wafers were too thick therefore they were not totally transparent in this region for the IR beam, which is often the case for ZSM-5 type zeolites.

The vibration bands in the C-H stretching region at 3094-3073-3039 cm^{-1} or 3070-3071 cm^{-1} are attributed to physisorbed benzene or chlorobenzene, and these bands can be removed by evacuation at room temperature.

Changes in the C-H out-of-plane region (2000-1800 cm^{-1}) are very similar independently what cations are located in the zeolitic channels. Thus, the various adsorption centers cannot be characterized by the shifts of these bands as it can be done for zeolite X- and Y-faujasite [68, 69].

The position of the vibration band $\nu_{19a,b}$ of benzene in the C-C stretching region changes, due to the type of cation introduced. It is located at $\nu_{19a,b}$=1479 cm^{-1} in the case of Pt- and Co-containing samples just like in the case of liquid

benzene. It splits into two bands in the case of Cu-containing zeolites, thus, the adsorption of benzene on Cu center results in the decrease of the D_{6h} symmetry of benzene, which is revealed in the energy separation of the originally degenerated vibrations. For chlorobenzene the energy of these vibrations is not degenerated originally and located at ν_{19a}=1480 cm^{-1} and ν_{19b}=1440 cm^{-1}.

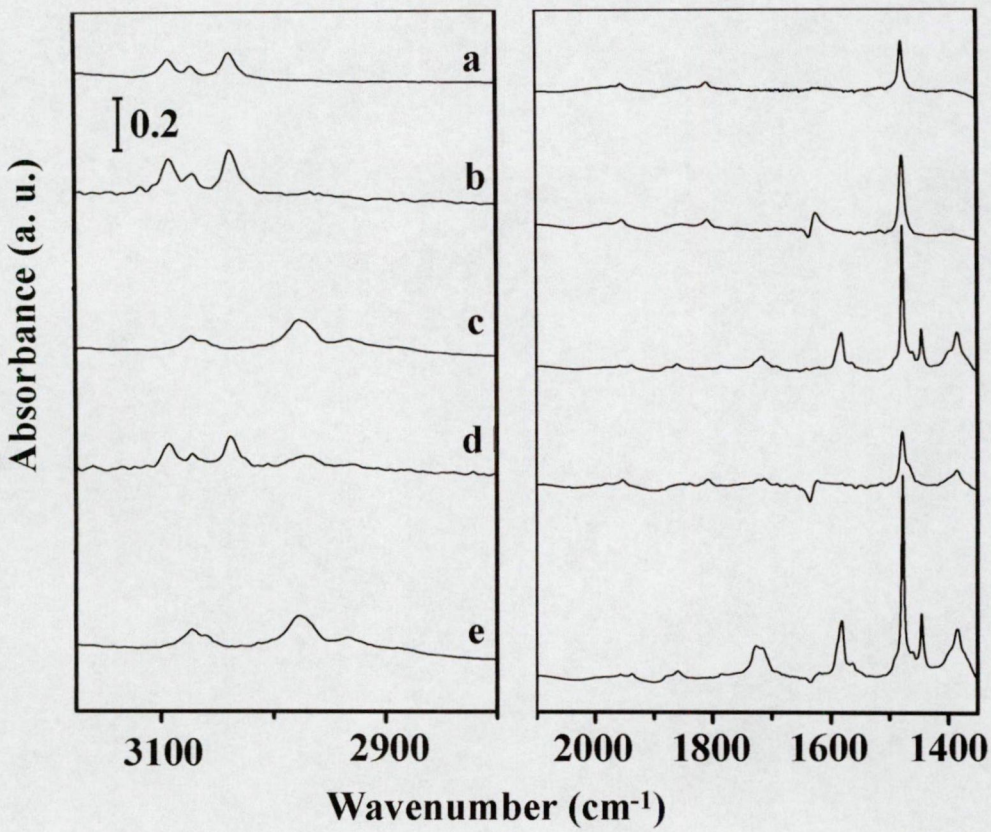

Figure 13. *IR spectra of adsorbed benzene on* ***a*** *PtZSM-5 (C) reduced in* H_2, ***b*** *CoZSM-5 (C),* ***d*** *CuZSM-5 (C) and chlorobenzene on* ***c*** *CoZSM-5 (C) and* ***e*** *CuZSM-5 (C)*

For adsorption of benzene and chlorobenzene new bands appear at 2975-2935 cm^{-1} and 1390 cm^{-1}. For benzene the bands can be detected only after evacuation. For chlorobenzene the bands are more intense. The increase in band intensities can be followed with time as can be seen in Figure 14.

The band at 1390 cm^{-1} had been assigned as benzene chemisorbed on platinum surface by Haaland [74, 75] and Palazov [77]. This band is the

combination of $\nu_4 + \nu_{17}$ normal vibrations ($b_{2g}+e_{2u}=E_{1u}$, combination bands, which are allowed in IR spectrum, having E_{1u} or A_{2u} symmetry [74]).

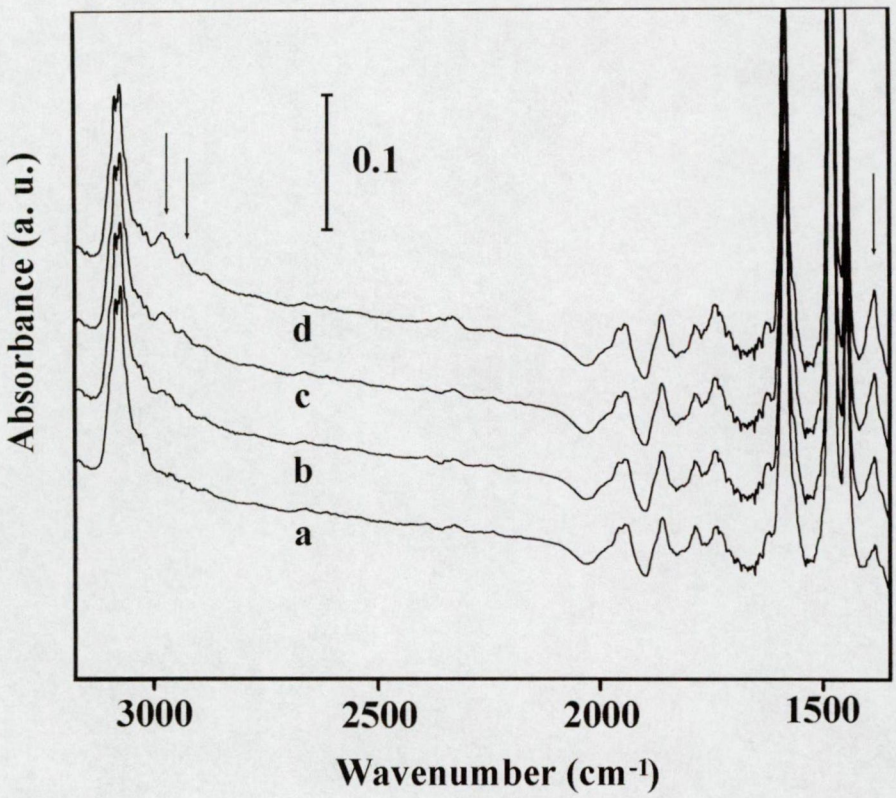

Figure 14. *IR spectra of adsorbed chlorobenzene on Pt,CoZSM-5 (C) reduced by H_2 after **a** 2 min **b** 5 min **c** 10 min **d** 30 min adsorption time*

Benzene chemisorbed on Pt/Al_2O_3 was detected in the C-H stretching region at 3050 cm^{-1} [74] or 3030-2947 cm^{-1} as π- and σ-bound benzene, respectively [75]. The bands appeared on Pt/Al_2O_3 in the 2900-2700 cm^{-1} region upon adsorption of a mixture of benzene and H_2 was attributed to chemisorbed cyclohexane formed on the platinum surface. In our case the bands at 2977-2935 cm^{-1} cannot be assigned as adsorbed cyclohexane because:

(i) Cyclohexane cannot be formed from chlorobenzene without the formation of HCl, and this compound was not detected.

(ii) After evacuation of physisorbed benzene or chlorobenzene the bands at 2975-2935 cm^{-1} are still present together with the band at 1390 cm^{-1}, while

the band at 1480 cm^{-1} is missing, which is characteristic for chemisorbed cyclohexane in the C-C stretching region.

(iii) For further evidence of the nature of adsorbed form the following experiment was carried out. After prolonged evacuation of the cell at room temperature (Figure 15, spectrum a), the cell was heated up to 373 K (spectrum b). In the spectra recorded the integrated intensity of the bands characteristic for the physisorbed benzene (3094-3073-3039 cm^{-1}) increased, while the integrated intensity of the bands of the adsorbed form decreased. After prolonged evacuation at 373 K the band of physisorbed benzene has disappeared (spectrum c).

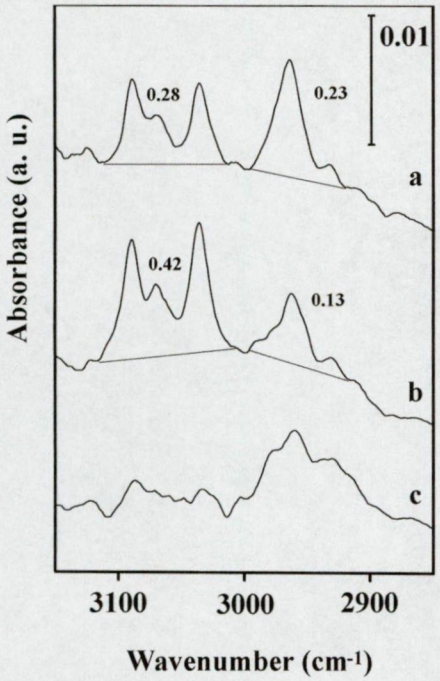

Figure 15. *IR spectra of adsorbed benzene on Pt,CoZSM-5 (C) reduced by $NaBH_4$* ***a*** *at 298 K after 30 min evacuation* ***b*** *at 373 K without evacuation* ***c*** *at 373 K after 30 min evacuation*

On the basis of these findings and the papers of Haaland [74,75] we assigned these bands as the chemisorbed π- and σ-bonded complexes of benzene and chlorobenzene on different metal centers. The observation of E_{1u} and B_{2u} vibration of chemisorbed benzene indicates that chemisorbed benzene is distorted to C_{3v} symmetry. The distortion is such that the chemisorbed benzene has alternating long and short C-C bonds, thus benzene approaches the classical Kekulé structure upon adsorption.

The bands of benzene and chlorobenzene are located similarly on bimetallic samples (see Figure 16).

On the Cu-containing samples the intensity of the chemisorbed bands is higher. By the examining these bands the different adsorption properties of mono- and bimetallic catalysts can be shown.

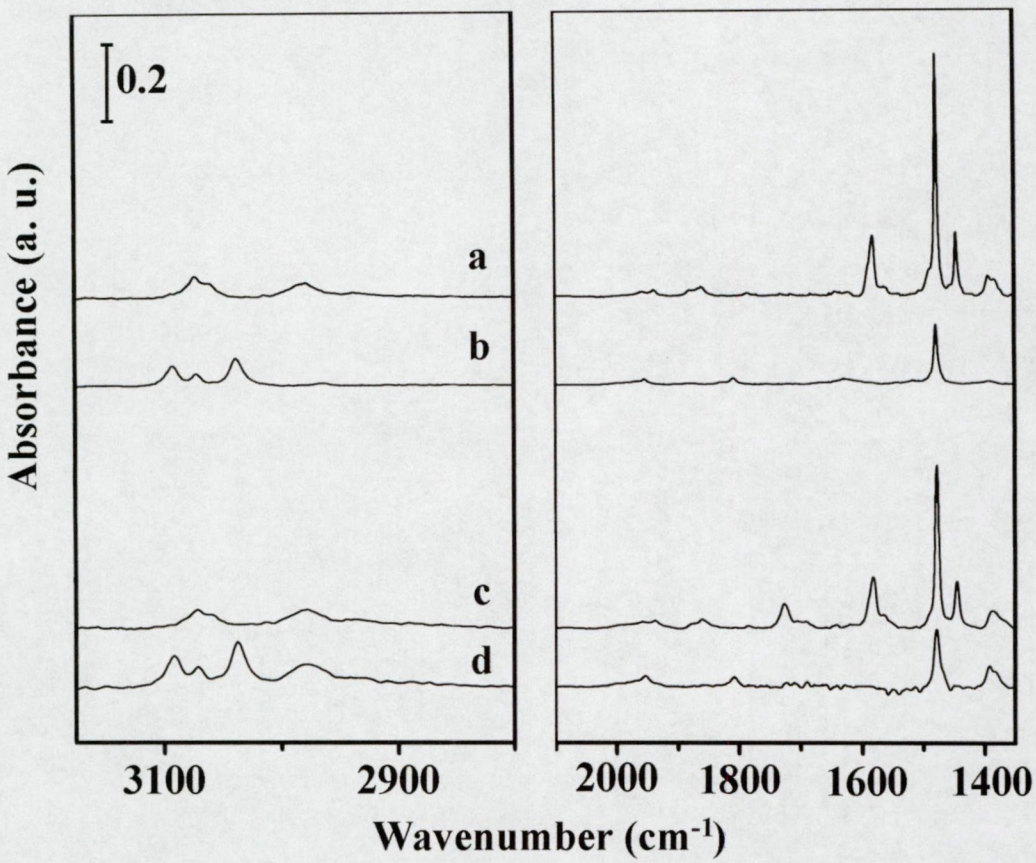

Figure 16. *IR spectra of adsorbed chlorobenzene on* ***a*** *Pt,CoZSM-5 (C) red. by H_2* ***c*** *Pt,CuZSM-5 (C) red. by H_2 and benzene on* ***b*** *Pt,CoZSM-5 (C) red. by H_2* ***d*** *Pt,CuZSM-5 (C) red. by H_2*

On Co- and PtZSM-5 samples the intensities of chemisorbed benzene bands are negligible, while for Pt,CoZSM-5 they appears, as can be seen in Figure 17.

From this follows that there are different adsorption centers in the bimetallic Pt,CoZSM-5 and in the monometallic Pt- or CoZSM-5 samples. The copresence of Pt and Co changes the adsorption properties of the metal cluster. Although, the bimetallic clusters were not investigated by commonly used surface science instruments (like EXAFS, low energy electron diffraction (LEED), field-ion microscopy (FIM) etc), by benzene adsorption we could detect the various properties of the bimetallic sample.

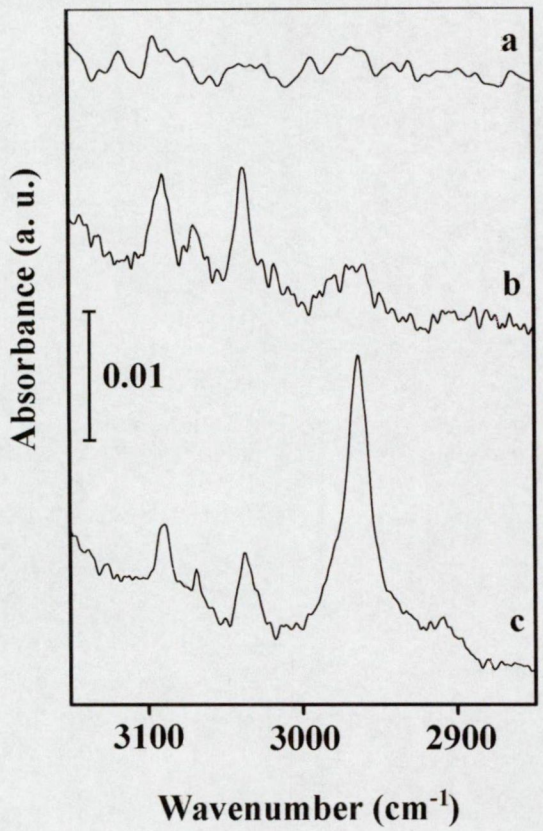

Figure 17. *IR spectra of adsorbed benzene on* ***a*** *CoZSM-5 (C)* ***b*** *PtZSM-5 (C) reduced by H_2 and* ***c*** *Pt,CoZSM-5 (C) reduced by H_2 at 298 K after 30 min evacuation*

5.5. Catalytic decomposition of chlorinated hydrocarbons

5.5.1. Hydrodechlorination of chlorobenzene

Chlorobenzene was taken as simple model reactant for studying the hydrodechlorination reaction of halogenated aromatic compounds with the purpose to investigate the mechanism and the influence of variable properties – acidity and metal loading – of the catalysts.

First, the reaction conditions were studied by IR spectroscopy. Then, in order to prove our conclusions certain catalysts, where the noticable effects can be seen, were investigated in a flow reactor system.

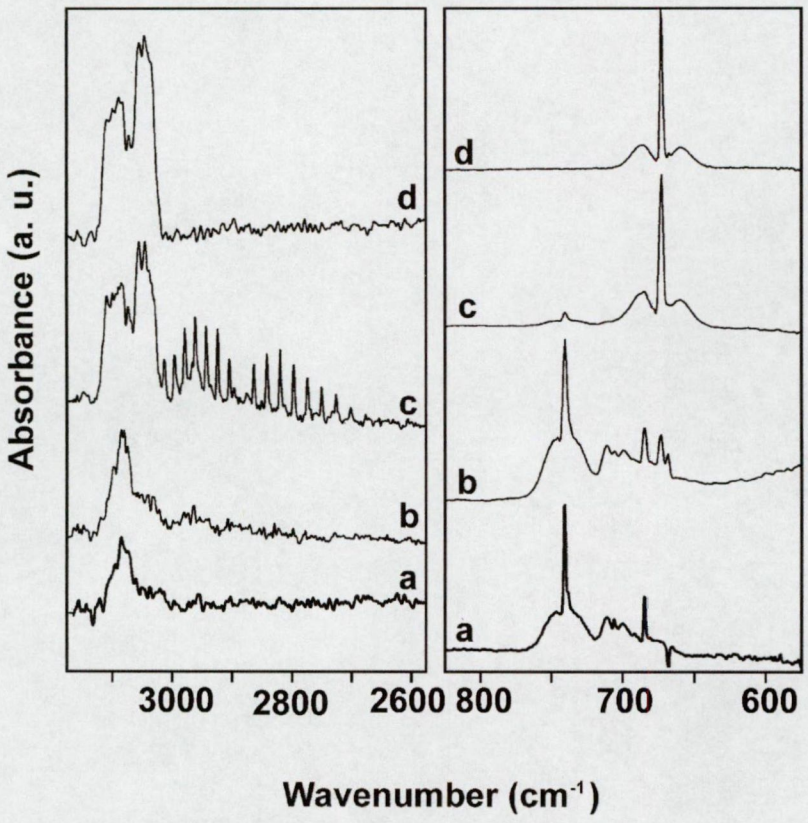

Figure 18. *Reference IR spectra of* ***a:*** *chlorobenzene* ***d****: benzene and IR spectra of gas phase products formed in hydrodechlorination reaction of chlorobenzene over Pt,CuZSM-5 (C) reduced in* H_2 ***b:*** *at 473 K and* ***c:*** *at 573 K*

In Figure 18 the IR spectra of gas-phase products formed in hydrodechlorination reaction over Pt,CuZSM-5 (C) reduced in H_2 at 473 K and 573 K, and the reference spectra of benzene and chlorobenzene can be found. The spectrum of gas phase at 473 K (spectrum b) is identical to that of chlorobenzene (spectrum a), thus no reaction takes place at this temperature. However, the spectrum changes significantly at 573 K (see spectrum c). The sturcture of vibration bands in C-C stretching (3094-3073-3039 cm^{-1}) or in C-H out-of-plane (673 cm^{-1}) region is corresponding to that of benzene (spectrum d). Besides, the vibration-rotation bands of gas-phase HCl can be detected, showing that HCl formed during the reaction desorbs from the catalyst and appears in the gas phase. Accordingly, the experiments were continued at 573 K and higher temperatures, since at least 573 K is necessary for the reaction to occur.

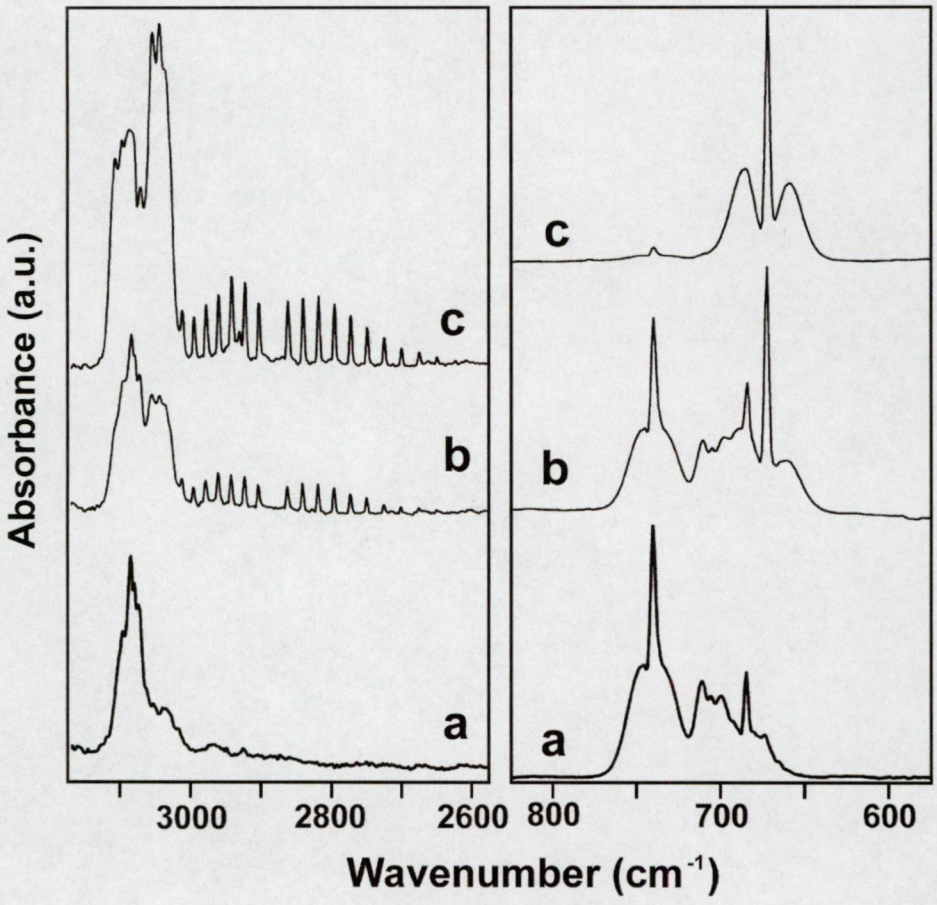

Figure 19. *IR spectra of gaseous products formed in hydrodechlorination reaction at 573 K over* ***a****: CuZSM-5 (C),* ***b:*** *Pt,CuZSM-5 (C) reduced in H_2 and* ***c:*** *PtZSM-5 (C) reduced in H_2*

In Figure 19 the IR spectra of the gas phase is presented in the hydrodechlorination reaction of chlorobenzene over CuZSM-5 (C), PtZSM-5 (C) reduced by hydrogen and Pt,CuZSM-5 (C) also reduced by hydrogen. CuZSM-5 catalyst (spectrum a) is inactive in hydrodechlorination reaction in a temperature range of 298-673 K, since the gas-phase spectrum is identical to that of chlorobenzene (for reference spectrum see Fig 18). The presence of platinum – noble metal component – is indispensable for the reaction to proceed. Although, on Pt- and Pt,CuZSM-5 catalysts the reaction took place to a different extent. Chlorobenzene partially transformed to benzene and HCl on Pt,CuZSM-5 (spectrum b), while the quantity of chlorobenzene in the gas phase is negligible after the reaction catalyzed by PtZSM-5 (spectrum c). A partial explanation for the difference is that the platinum content of PtZSM-5 (C) is higher than that of Pt,CuZSM-5 (C). On the other hand, Cu can dilute the Pt island in the bimetallic particle and may cause the decreased activity [99].

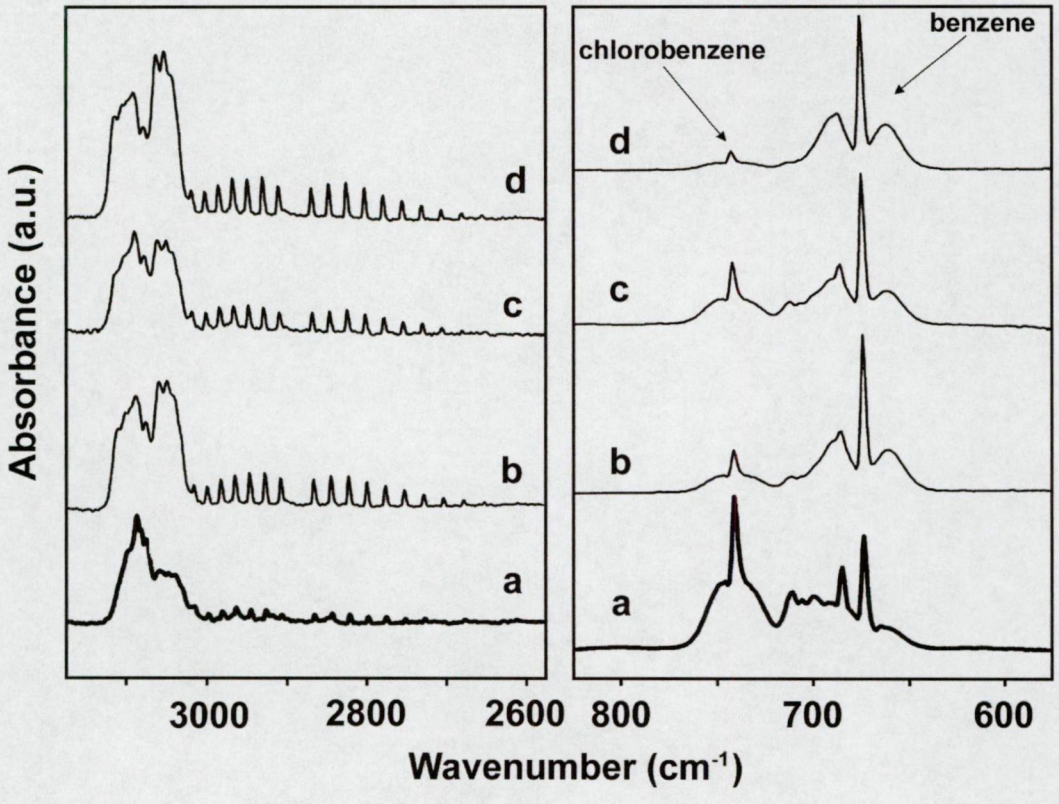

Figure 20. *IR spectra of gaseous products formed in hydrodechlorination reaction at 573 K over* ***a:*** *Pt,CoZSM-5 (C) red. in $NaBH_4$,* ***b****: Pt,CoZSM-5 (C) red. in H_2 and* ***c:*** *Pt,CuZSM-5 (C) red. in $NaBH_4$* ***d****: Pt,CuZSM-5 (C) red. in H_2*

The effect of the different reduction methods on the catalytic activity can be seen in Figure 20 for Pt,Cu- and Pt,CoZSM-5 (C) catalysts. The catalysts, reduced by hydrogen, thus, having Brønsted acidity, show higher activity in hydrodechlorination of chlorobenzene – as can be easily followed by the changing vibration bands characteristic for chlorobenzene or benzene in the C-H out-of-plane region – than those, which were reduced by $NaBH_4$.

On the basis of preliminary IR studies PtZSM-5 (C) reduced by H_2 and Pt,CuZSM-5 (C) reduced by H_2 and Pt,CuZSM-5 (C) reduced by $NaBH_4$ were chosen for catalytic tests. In a flow reactor system, in the trapped reaction mixture at outlet only benzene and chlorobenzene were detected by GC. Conversion values gained for 100-minute runs are listed in Table 6 and the Arrhenius plots are seen in Figure 21. Results are in accordance with those received from IR measurements: (i) PtZSM-5 (C) shows the highest activity in hydrodechlorination; and (ii) the reaction is acid sensitive. It is probable that H_2 dissociated on platinum spilled over onto the acidic support, and reacted with chlorobenzene weakly bound on the surface. Onto neutral support the hydrogen spillover does not take place

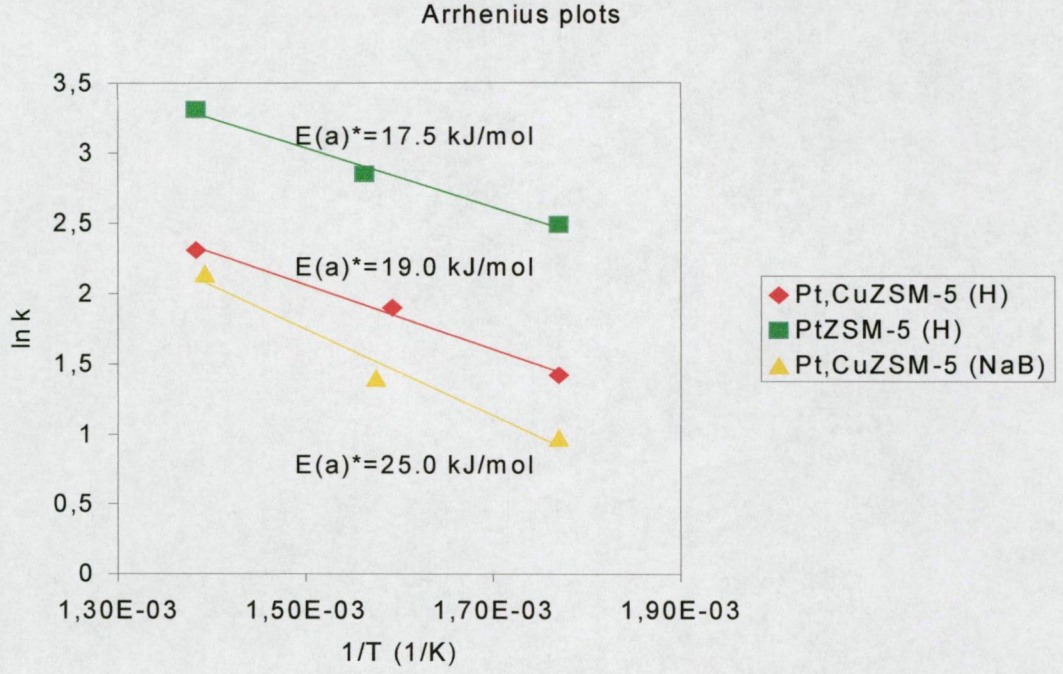

Figure 21. *Arrhenius plots for hydrodechlorination reaction of chlorobenzene over different catalysts*
(H): *reduced by H_2 and* ***(NaB):*** *reduced by $NaBH_4$*
E(a)*: *Apparent activation energy*

[114].

Sample	Conversion (%)		
	at 573 K	at 643 K	at 723 K
PtZSM-5 (C) red. in H_2	70	78	88
Pt,CuZSM-5 (C) red. in H_2	33	45	54
Pt,CuZSM-5 (C) red. in $NaBH_4$	23	30	48

Table 6. *Conversion values gained for 100-minute runs in hydrodechlorination reaction of chlorobenzene over different catalysts*

PtZSM-5 (C) and Pt,CuZSM-5 (C) catalysts, both reduced by H_2, were tested in time in order to see the effect of HCl adsorbed or the prolonged heat treatment on the catalytic activity. In Figure 22 the conversion received are presented vs. time. As can be seen both catalysts keep their high activity during the five times longer testing time. The catalysts were checked by TEM. Further agglomeration and migration towards the outer surface of metallic particles during the reaction were negligible.

On the basis of these findings Pt- and Pt,CuZSM-5 catalysts reduced by H_2 are active and selective in the hydrodechlorination of chlorobenzene to benzene, and preserves their high activity on increasing time on stream. It is worth expanding the research of the noble metal loaded ZSM-5 zeolites to hydrodechlorination reactions of polychlorinated aromatics, or other hydroprocessing reactions like hydrodesulphurisation, hydrodenitrogenation reactions and hydrodechlorination in a mixture of chlorobenzene pyridine and thiophene.

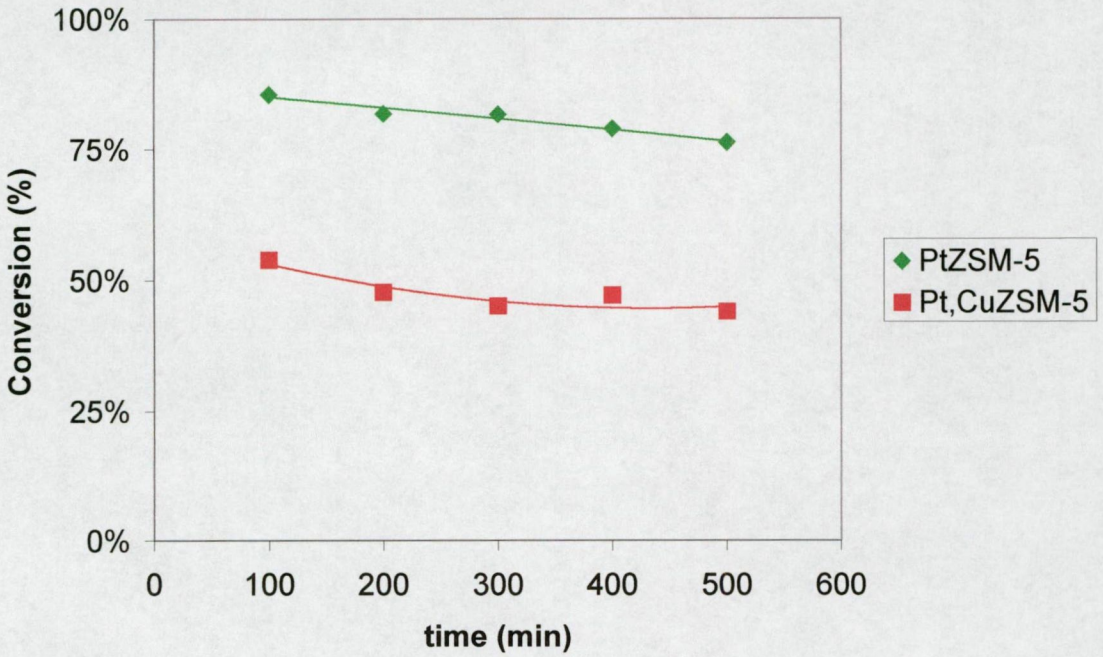

Figure 22. *Hydrodechlorination reaction of chlorobenzene over Pt- and Pt-CuZSM-5 (C) reduced by H_2 at 723 K*

5.5.2. Transformation of CCl_4 under oxidative, neutral and reductive conditions

Carbon tetrachloride can be regarded as model compound of CFCs (CFC-10). The investigation of its decomposition reaction allows the elucidation the chemistry of C-Cl bond cleavage in alkyl halogenides including CFCs.

5.5.2.1. Decomposition of CCl_4 under oxidative and neutral conditions

In Figure 24 IR spectra of gas phase products formed in the decomposition of carbon tetrachloride in neutral (N_2) and oxidative (O_2) atmosphere over PtZSM-5 (B) and Pt-CoZSM-5 (B) zeolites, both reduced in hydrogen, are

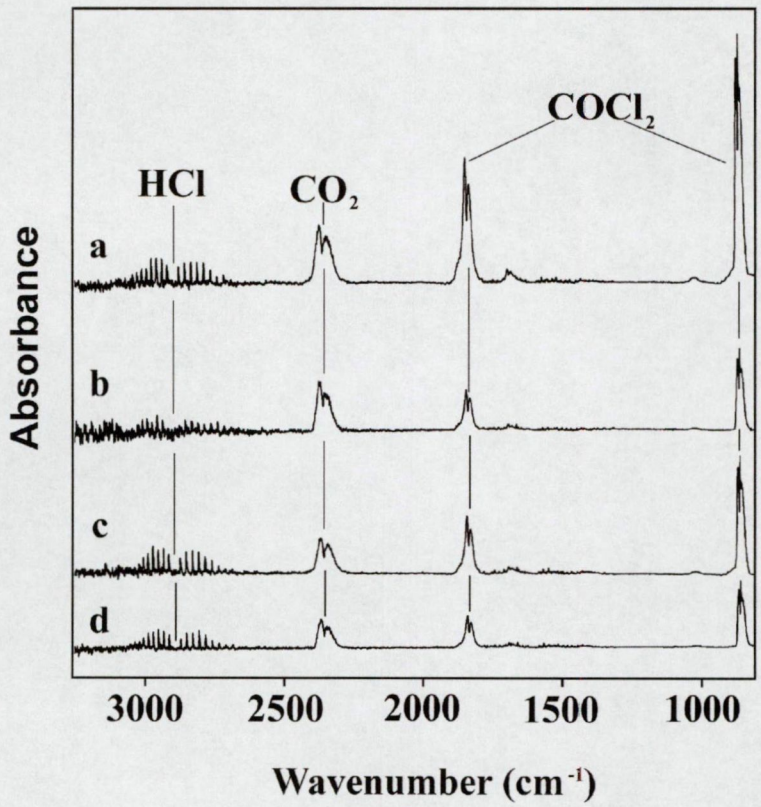

Figure 23. *IR spectra of products formed in transformation of CCl_4 in oxidative media (O_2) on **a** Pt- (B) (red. in H_2) and **b** Pt,CoZSM-5 (B) (red. in H_2) and in inert media (N_2) on **c** Pt- (B) (red. in H_2) and **d** Pt,CoZSM-5 (B) (red. in H_2) catalysts*

depicted. It is seen that the products in the two media are nearly identical. Phosgene, CO_2 and HCl are the main products giving rise to bands at 1750, 2400 and 2900 cm^{-1}, respectively. The concentration of these compounds increases with reaction temperature. In the presence of oxygen in the reacting mixture increase the reaction rate, which is manifested in the increasing amount of oxygenated products ($COCl_2$ and CO_2), and slows down the dealumination of zeolite framework [115].

The chlorine atoms of CCl_4 react with the Al of zeolites coordinated tetrahedrally resulting the formation of octahedrally coordinated extraframework Al (see scheme 4 [116]). This transformation results in the formation of zeolite with vacancies in their skeleton. As a consequence of these transformations, the crystal structure of the zeolite collapses rapidly for zeolites with low Si/Al ratios, while for zeolites with high Si/Al ratios the collision is retarded and can be hardly detected. The zeolite should be, therefore, regarded as a reaction partner rather than a catalyst under oxidative and neutral conditions.

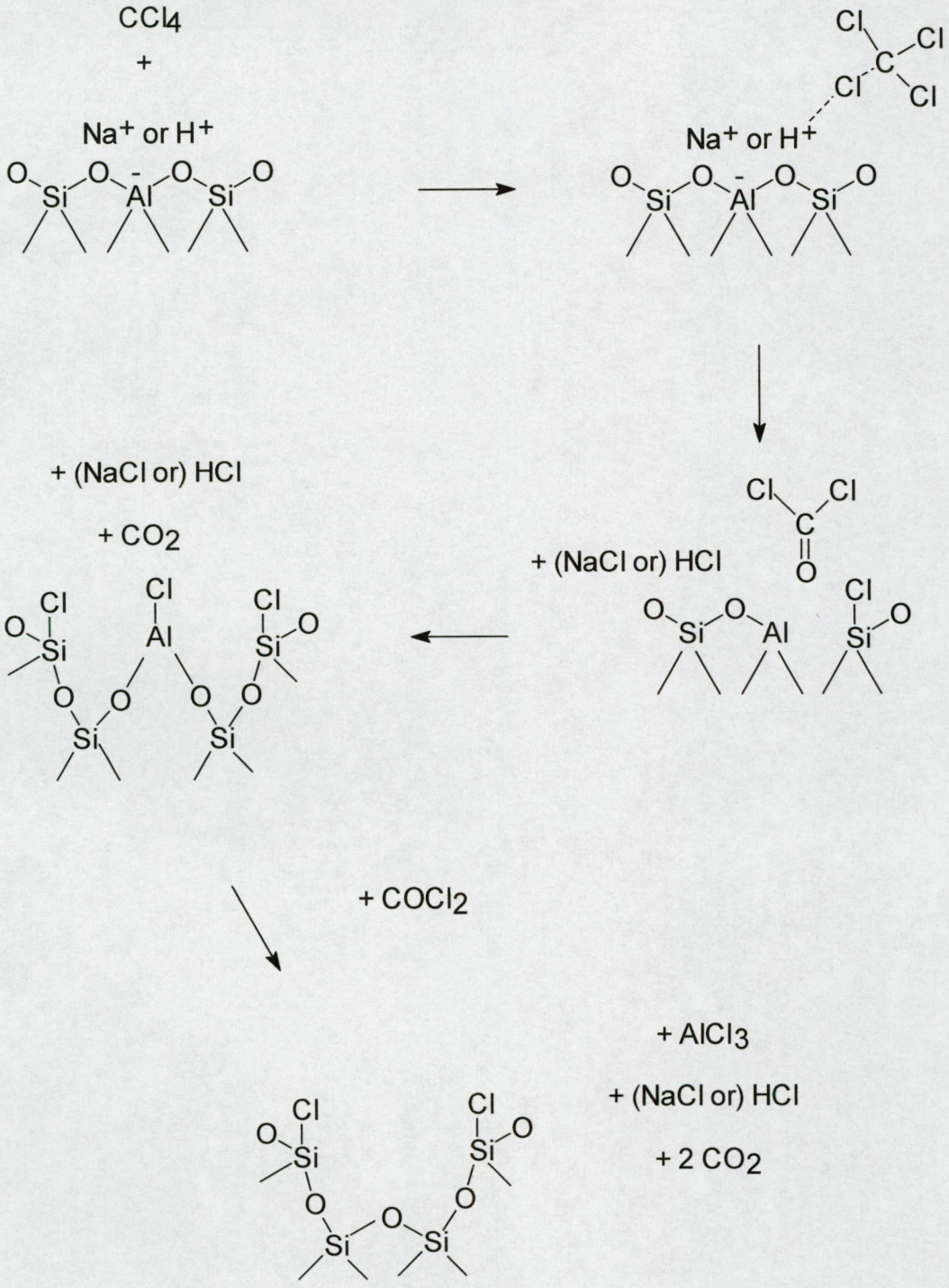

Scheme 4. *Decomposition of CCl_4 over zeolites in oxidative or inert media*

5.5.2.2. Hydrodechlorination of CCl_4 under reductive conditions

Figure 24 shows the spectra of the products obtained over Pt,CoZSM-5 (B) samples reduced in different ways and reacted in reductive conditions.

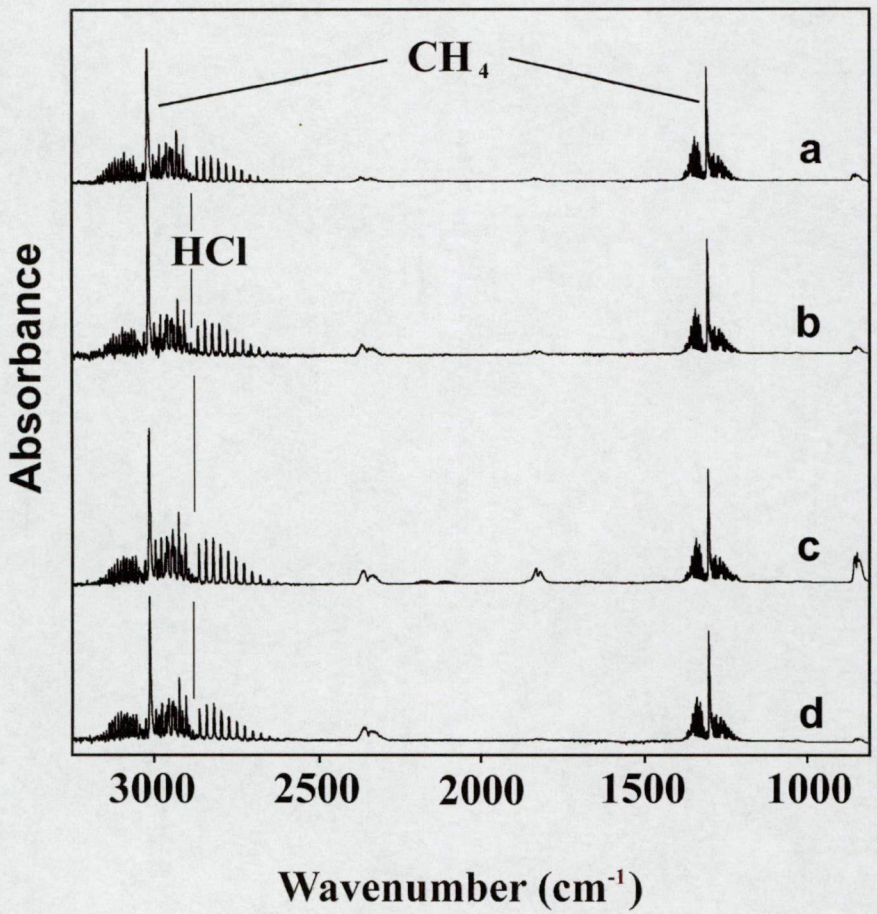

Figure 24. *IR spectra of products formed in transformation of CCl_4 in reductive media (H_2) on* ***a*** *Pt- (B) (red. in H_2) and* ***b*** *Pt,CoZSM-5 (B) (red. in H_2)* ***c*** *Pt- (B) (red. in $NaBH_4$) and* ***d*** *Pt,CoZSM-5 (B) (red. in $NaBH_4$) catalysts*

The difference in the product distribution compared to neutral and oxidative conditions is clearly seen. While in neutral, and oxidative atmosphere phosgene, CO_2 and HCl are the main products, in the experiments performed in reductive atmosphere methane and HCl form. Among the products partially chlorinated methane derivatives – such as chloro methane, dichloro methane or chloroform – or C-C coupled hydrocarbon derivatives have not been detected. From this follows

that substantial difference should be in the mechanism of the reaction taking place under various conditions. It is also remarkable, that the products are present in almost identical concentrations for both hydrogen and $NaBH_4$ reduced samples. This result shows the negligible importance of the reduction method and acidity in the reaction performed in hydrogen. As we mentioned before, acidity played an important role at the hydrodechlorination reactions of aromatic hydrocarbons. In the case of CCl_4 the importance of the acidity became insignificant. From this follows that the metal function of (Pt, or Pt,Co) is predominant in the hydrodechlorination reaction of carbon tetrachloride.

IR spectra taken on the spent zeolite samples and depicted in Figure 25 show unequivocally that no crystal destruction and/or significant dealumination of the zeolite framework occurred in the reactions performed hydrogen atmosphere. No indication of the IR band attributed to framework vacancies is seen at 930 cm^{-1} in the spectra presented. We can conclude that bimetallic zeolites prepared on the basis of high modulus materials such as ZSM-5 are promising specimens for application in hydrodechlorination reactions. The use of ZSM-5 type zeolites supplies a new, promising way for the preparation of catalysts with prolonged activity in hydrodechlorination reaction, while Kim et al. claimed fast deactivation of Pt/NaY zeolite [117]. On the basis of these findings the research of hydrodechlorination can be extended

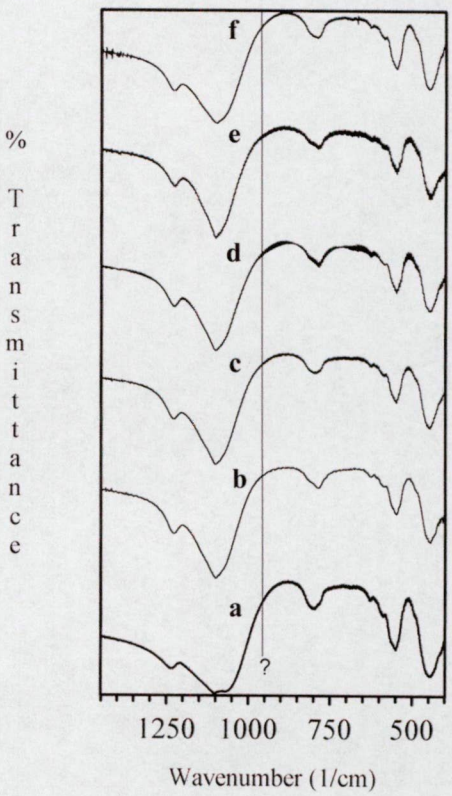

Figure 25. *IR spectra of the spent catalysts,* ***a:*** *Na,HZSM-5,* ***b:*** *PtZSM-5 (H_2) reaction in N_2 media,* ***c:*** *PtZSM-5 ($NaBH_4$) reaction in H_2 media,* ***d:*** *PtZSM-5 (H_2) reaction in H_2 media,* ***e:*** *PtZSM-5 ($NaBH_4$) reaction in N_2 media,* ***f:*** *PtZSM-5 (H_2) reaction in O_2 media*

to the wide scale of CFCs. Since the C-F bond is stronger this way the C-Cl bond could be cleave without attacking the C-F bond.

6. SUMMARY

One or two metal loaded (Pt, Cu or Co and Pt,Cu or Pt,Co) ZSM-5 type zeolites were synthesized, characterized and investigated in C-Cl bond cleavage reactions.

The results show that each sample preserved its original structure upon different treatments.

Brønsted acid centers were generated (i) when transition metal ion is exchanged into zeolite with high modulus or (ii) if H_2 is used for reduction of exchanged cations.

Using $NaBH_4$ as reducing agent reduction proceeded without generation of Brønsted acid sites.

Combining the two methods tailor-made acidity generation may be performed and, simultaneously, complete reduction can be achieved.

The concentration of the metal components on the outer surface of the samples varied upon different reduction procedures.

For Pt,CuZSM-5 sample considerable increase of Pt was found after reduction with $NaBH_4$, while this treatment did not affect the state of platinum in the cobalt-containing sample. Enhanced surface concentrations of cobalt and copper were observed for samples reduced by $NaBH_4$.

Upon benzene and chlorobenzene adsorption the bands in the range of zeolitic OH (3500-4000 cm^{-1}) and benzene (or chlorobenzene) C-H out-of-plane region (2000-1800 cm^{-1}) did not shift characteristically for the metals inserted in ZSM-5 zeolite matrix.

The degenerated band pair found in C-C stretching region split into two bands upon adsorption on Cu centers. It indicates the decrease of the D_{6h} symmetry of the benzene.

We assigned the bands at 2977 and 2935 cm^{-1} as the chemisorbed π- and σ-bonded complexes of benzene and chlorobenzene on different metal centers. The presence of band at 1390 cm^{-1} characteristic for chemisorbed benzene (or chlorobenzene) shores up our assertion. The observation of E_{1u} and B_{2u} vibration of chemisorbed benzene indicates that it is distorted to C_{3v} symmetry. Distortion

occurs in a way that chemisorbed benzene has alternating long and short C-C bonds, thus, benzene approaches the classical Kekulé structure upon adsorption.

In the hydrodechlorination reaction of chlorobenzene the Pt content of catalysts has indispensable role. PtZSM-5 showed higher activity than the bimetallic (Pt,Cu and Pt,CoZSM-5) zeolites.

It was showed that Brønsted acidity plays significant role in the reaction mechanism. According to our assumptions, the hydrogen atom dissociated on platinum surface spills over to the acidic support where chlorobenzene is weakly bound.

The activity of Pt- and Pt,CuZSM-5 catalysts did not decrease significantly, the metals did not sinter and migrate towards the outer surface, and the structure of the zeolites did not collapse.

The completely different product distribution observed in the decomposition reaction of CCl_4 under neutral, oxidative or reductive conditions suggest two different reaction mechanisms.

Under neutral or oxidative conditions the carbon tetrachloride reacts with the zeolite irrespective it metal content or Brønsted acidity. This reaction leads to fast dealumination of the zeolite resulting in the collapse of the crystal structure.

Under reductive conditions hydrodechlorination takes place as the main reaction producing methane and HCl. It seems to be promising to apply Pt- and Pt,CoZSM-5 catalysts to produce HFCs from CFCs.

7. MAGYAR NYELVŰ ÖSSZEFOGLALÓ (Hungarian Summary)

Cu-, Co-, PtZSM-5-t és ezek kétfémes változatait (Pt,Cu- és Pt,CoZSM-5) állítottuk elő, jellemeztük különböző fizikai és kémiai módszerekkel, továbbá megvizsgáltuk katalitikus aktivitásukat szén-klór kötés hasítási reakciókban.

A szerkezetvizsgálat során kapott eredmények alapján megállapítottuk, hogy a különböző (elő)kezelések hatására az eredeti ZSM-5 struktúrában nem következett be károsodás.

Kimutattuk, hogy redukció hatására a fémionok fémmé redukálódnak, azonban a redukálószer minőségétől függően a katalizátorok eltérő savasságot mutatnak. Amennyiben a redukciót hidrogénnel hajtottuk végre, Brønsted savcentrumot generáltunk, ha nátrium borohidriddel végeztük, akkor a fém teljes redukciója lejátszódott Brønsted savcentrumok keletkezése nélkül. Ez utóbbi esetben az ioncsere pozíciókat a redukció után Na^+-ionok foglalják el. Ezen eredmények alapján feltételezhető, hogy a két redukciós módszer kombinálásával a zeolithordozós fémkatalizátor savassága előre tervezett módon alakítható, ennek segítségével pedig egy kulcskérdés, a Brønsted savasság katalitikus reakciókban betöltött szerepe tisztázható.

A potenciális katalizátorok adszorpciós tulajdonságait benzol és klórbenzol próbamolekulák segítségével vizsgáltuk. Rézion-tartalmú minták esetén azt tapasztaltuk, hogy az adszorpció során a benzol eredetileg degenerált sávpárja felhasad ($\nu_{19a,19b}$ = 1482 cm^{-1}), mutatva a D_{6h} szimmetria megszűnését. Két, az adszorpció során megjelent sávot azonosítottunk (ν = 2977 cm^{-1} és ν = 2935 cm^{-1}), mint a fémcentrumokon, illetve a fémionokon kemiszorbeálódott benzol, illetve klórbenzol. Vizsgálataink során a Co- és PtZSM-5 katalizátoron a kemiszorbeálódott benzolt nem észleltük, azonban a kétfémes változaton megjelentek az erre jellemző sávok. Mindezek alapján a kétfémes mintában ötvözet jelenlétét feltételezzük.

Vizsgálataink távlati célja volt klór-tartalmú szénhidrogének hidrogén áramban való bontásához alkalmas katalizátor előállítása. Tanulmányoztuk tehát az egy- és kétfémes zeolitok katalitikus aktivitását klórbenzol, illetve széntetraklorid modellanyagokat felhasználva.

Tapasztalataink alapján a nemesfém jelenléte a katalizátorban nélkülözhetetlen a szén-klór kötés hidrogenolíziséhez mind klórbenzol, mind pedig széntetraklorid esetén.

Kimutattuk, hogy a klórbenzol hidrodeklórozása során a katalizátorminták Brønsted savassága is fontos szerepet játszik. Irodalmi előzmények alapján feltételezzük, hogy a nemesfémen disszociálódó hidrogén képes a savas hordozóra vándorolni, ahol a klórbenzol gyengén kötődik, míg a semleges hordozón ez nem történik meg. Fárasztási kísérleteinkben a hidrogénnel redukált Pt- és Pt,CuZSM-5 katalizátoroknak nem csökkent jelentősen az aktivitásuk, emellett a reakció hatására nem történt meg a fémrészecskék nagymértékű agglomerizációja, a felület irányába történő vándorlása, illetve a zeolitrács összeomlása. Ezen eredmények alapján érdemes e katalizátorokat a reakcióban hosszabb ideig tesztelni, illetve a reaktánsok körét a poliklórozott aromás szénhidrogének körére kiterjeszteni.

A széntetraklorid, mint freon modellvegyület, átalakítási reakciója során inert és oxidatív közegben teljesen eltérő termékösszetételt kaptunk a reduktív közeghez viszonyítva. Megállapítottuk, hogy N_2 és O_2 áramban a CCl_4 elreagál a zeolitráccsal, függetlenül annak fémtartalmától, illetve Brønsted savasságától. Reduktív közegben – H_2 áramban – azonban a CCl_4 katalitikus hidrodeklórozása játszódik le CH_4-t és HCl-t eredményezve, a zeolitrács tapasztalható mértékű károsodása nélkül.

A kísérleteket érdemes kiterjeszteni a hidrogént nem tartalmazó – így a környezetre ártalmas – freonok széles körének vizsgálatára, ugyanis a reakciókörülmények optimális megválasztása esetén lehetőség nyílhat a hidrogént tartalmazó helyettesítő freonok előállítására.

8. REFERENCES

1 J. B.Nagy, P. Bodart, I. Hannus, I. Kiricsi: Synthesis, characterization and use of zeolitic microporous materials", DecaGen Ltd. (1998) 7.

2 J. B.Nagy, I. Hannus, I. Kiricsi: „Nanoclusters in zeolites", John Wiley (ed), Weinheim (1998) 389.

3 W.M.H. Sachtler, Z. Zhang: Advances in Catalysis, 39 (1993) 129.

4 N.Y. Chen, T.F. Degnan: Chem. Eng. Prog., 84 (1988) 32.

5 M. Taramasso, G. Perego, B. Notari: Proc. Int. Conf. Zeolites, 5th Naples, (1980) 40.

6 V.I. Parvulescu, P. Grange, B. Delmon: Catal. Today, 46 (1998) 233.

7 G. Price, V. Kanazirev: J. Catal., 126 (1990) 267.

8 G.A. Mills, H. Heinemann, T.H. Millikan, A.G. Oblad: Ing. Eng. Chem., 45 (1953) 134.

9 F. Ribeiro, C. Marcilly, M. Guisnet: J. Catal., 78 (1982) 275.

10 S.T. Homeyer, Z. Karpinski, W.M.H. Sachtler: J. Catal., 123 (1990) 60.

11 W.M.H. Sachtler, A.Y Stakheev: Catal. Today, 12 (1992) 283.

12 R.A. Dalla Betta, M. Boudart: Proc. Int. Congr. Catal. 5th (1973) 1329.

13 L. Guczi, I. Kiricsi: Appl. Catal. A, 186 (1999) 375.

14 G. Lu, Z. Zsoldos, Zs. Koppány, L. Guczi: Catal. Lett., 24 (1993) 15.

15 Z. Zsoldos, G. Vass, G. Lu, L. Guczi: Appl. Surf. Sci., 78 (1994) 467.

16 L. Guczi, G. Lu, Z. Zsoldos, Zs. Koppány: Stud. Surf. Sci. Catal., 84 (1994) 949.

17 T.-A. Lin, L.H. Schwartz, J.B. Butt: J. Catal., 97 (1986) 177

18 D.W. Breck: „Zeolite Molcular Sieves", Wiley, Interscience, New York (1974) Chap. 7.

19 W. Romanowski, J.M. Jablonski in: „Catalysis on Zeolites",D. Kalló, Kh. M. Minachev (Eds.), Akadémia Kiadó, Budapest (1988) Chap. 10.

20 B. Whichterlova, L. Kubelkova, J. Novakova in: „Catalysis on Zeolites",D. Kalló, Kh. M. Minachev (Eds.), Akadémia Kiadó, Budapest (1988) Chap. 11.

21 N.P. Davidova, in: „Catalysis on Zeolites",D. Kalló, Kh. M. Minachev (Eds.), Akadémia Kiadó, Budapest (1988) Chap. 12.

22 Z. Zhang, W.M.H. Sachtler: J. Chem. Soc. Faraday Trans., 86 (1990) 2313.

23 H. G. Karge: Stud. Surf. Sci. Catal., 105 (1997) 1901.

24 V. Schünemann, H. Trevino, W.M.H. Sachtler, K. Fogash, J.A. Dumesic: J. Phys. Chem., 99 (1995) 1317.

25 T. M. Tri, J. Massardier, P. Gallezot, B. Imelik: J. Catal., 85 (1984) 244.

26 L. Riekert: Ber. Bungsenges. Phys. Chem., 73 (1969) 3.

27 A. Béres, I. Hannus, I. Kiricsi: J. Thermal Anal., 46 (1996) 1301.

28 A. Béres, I. Hannus, I. Kiricsi: J. Thermal Anal., 47 (1996) 419.

29 I. Hannus, A. Béres, J. B.Nagy, J. Halász, I. Kiricsi: J. Mol. Struct., 410-411 (1997) 43.

30 S.T. Homeyer, Z. Karpinski, W.M.H. Sachtler: J. Catal., 117 (1989), 91.

31 M.S. Tzou, B.K. Teo, W.H.M. Sachtler: J. Catal., 113 (1988) 220.

32 P. Gallezot: Catal. Rev. Sci. Eng., 20 (1979) 121.

33 L. Guczi, Z. Kónya, Zs. Koppány, G. Stefler, I. Kiricsi: Catal. Lett. 44 (1997) 7.

34 D.W. Breck, C.R. Castor, R.M. Milton: US Patent 3,013,990 (1961)

35 C. Naccache, Y.B Taarit: J. Catal., 22 (1971) 171.

36 J.A. Rabo, C. L. Angell, P.H. Kasai, V. Schomaker: Disc. Faraday Soc., 41 (1966) 328.

37 P.H. Kasai, R.J. Bishop: J. Am. Chem. Soc., 94 (1972) 5560.

38 I. Manninger, Z. Paál, B. Tesche, U. Klengler, J. Halász, I. Kiricsi: J. Mol. Catal., 64 (1991) 361.

39 P.A. Jacobs: „Carbiniogenic Activity of Zeolites", Elsevier, Amsterdam, (1977) 183.

40 H.J. Jiang, M.S. Tzou, W.M.H. Sachtler: Catal. Lett., 1 (1988) 99.

41 M. Suzuki, K. Tsutsumi, H. Takahashi, Y. Saito: Zeolites, 8 (1988) 284.

42 M. Suzuki, K. Tsutsumi, H. Takahashi, Y. Saito: Zeolites, 8 (1988) 381.

43 G. Lu, T. Hoffer, G. Guczi: Catal. Lett., 14 (1992) 207.

44 L. Guczi, D. Bazin: Appl. Catal. A, 188 (1999) 163.

45 L. Guczi, Zs. Koppány, K.V. Sarma, L. Borkó, I Kiricsi: Stud. Surf. Sci. Catal., 105 (1997) 861.

46 J.A. Rodriguez, D.W. Goodman: J. Phys. Chem, 95 (1991) 4196.

47 E. Blomsma, J.A. Martens, P.A. Jacobs: J. Catal., 165 (1997) 241.

48 O.B. Yang, S.I. Woo, Y.G. Kim: Appl. Catal. A, 115 (1994) 229.

49 P. Meriaudeau, C. Naccache, A. Thangaraj, C.L. Bianchi, R. Carli, S. Narayanan: J. Catal. 152 (1995) 313.

50 J. Elliott, J.H. Lunsford: J. Catal., 57 (1979) 11.

51 Z. Karpinski, Z. Zhang, W.M.H. Sachtler: Catal. Lett., 13 (1992) 123.

52 T.R.O. Souza, S.M.O. Brito, H.M.C. Andrade: Appl. Catal. A, 178 (1999) 7.

53 E.S. Shpiro, O.O. Tkachenko, N.I. Jaeger, G. Schultz-Ekloff, W. Grünert: J. Phys. Chem B, 102 (1998) 3798.

54 S.E. Maisuls, S. Feast, K. Seshan, J.G. van Ommen, J. A. Lercher: Proc. of 12th Int. Zeolite Conf. (1999) 2889.

55 S.E. Maisuls, K. Seshan, S. Feast, J.A. Lercher: Appl. Catal. B, 29 (2001) 69.

56 L. Gutierrez, A. Boix, J. Petunchi: Catal. Today, 544 (1999) 451.

57 L. Gutierrez, E.A. Lombardo, J. Petunchi: Appl. Catal. A, 194-195 (2000) 169.

58 G. Moretti, W.M.H. Sachtler: J. Catal., 15 (1989) 205.

59 M-S. Tzou, M. Kusunoki, K. Asakura, H. Kuroda, G. Moretti, W.M.H. Sachtler: J. Phys. Chem., 95 (1991) 5210.

60 G. Lu, L. Guczi: Zeolites and Microporous Crystals (ed. Y. Izumi) 1994, 347 (Kodansha, Tokyo)

61 G. Lu, L. Guczi: Stud. Surf. Sci. Catal., 94 (1995) 171.

62 Atlas of zeolites, Zeolites, 10 (1990) 443 S, 445 S.

63 P. Fejes, I. Hannus, I. Kiricsi: Zeolites, 4 (1984) 73.

64 S.J. Gregg, K.S.W. Sing: „Adsorption surface area and porosity", Academic Press, London & New York, 1967, Ch. 1, 5.

65 S.J. Gregg, K.S.W. Sing: „Adsorption surface area and porosity", Academic Press, London & New York, 1967, Ch. 2, 35.

66 E.P. Parry: J. Catal., 2 (1963) 371.

67 P. Fejes, D. Kalló: Acta Chim. Hung., 39 (1963) 213.

68 B.L. Su, D. Barthomeuf: Zeolites 15, (1995) 470.

69 A. de Mallmann, D. Barthomeuf: Zeolites 8 (1988) 292.

70 B. Gil, E. Broclawik, J. Datka, J. Klinowski: J. Phys. Chem., 98 (1994) 930.

71 A. Jentys, J. A. Lercher: Stud. Surf. Sci. Catal., 46 (1989) 585.

72 K. Weiss, S. Gelbert, M. Wühn, H. Awadepohl, Ch. Wöll: J. Vac. Sci. Technol. A, 16 (1998) 1017.

73 S. Haq, D. A. King: J. Phys. Chem., 100 (1996) 16957.

74 D. M. Haaland: Surf. Sci., 102 (1981) 405.

75 D. M. Haaland, Surf. Sci., 111 (1981) 555.

76 M. Primet, J.M. Basset, M.V. Mathieu, M. Prettre: J. Catal, 29 (1973) 213.

77 A. Palazov: J. Catal., 30 (1973) 13.

78 J. Erelens, S. H. Eggink-du Bruk: J. Catal., 15 (1969) 62.

79 M.J. Molina, F S. Rowland: Nature, 249 (1974) 810.

80 Y.Takita, M. Ninomiya, R. Matsuzaki, H. Wakamatsu, H. Nishiguchi, T. Ishihara: Phys. Chem. Chem. Phys, 1 (1999) 2367.

81 S. Okazaki A., Kurosaki: Chem. Lett. (1989) 389.

82 S. Karmakar, H.L. Greene: J. Catal., 103 (1987) 399.

83 E. Kemnitz, A. Hess, G. Rother, S. Troyanov: J. Catal, 159 (1996) 332.

84 G.M. Bickle, T. Suzuki, Y. Mitarai: Appl. Catal. B, 4 (1994) 141.

85 Z. Kónya, I. Hannus, I. Kiricsi: Appl. Catal. B, 8 (1996) 391.

86 I. Hannus, Z. Kónya, J. B.Nagy, I. Kiricsi: J. Mol. Struct., 410-411 (1997) 89.

87 I. Hannus, Z. Kónya, J. B.Nagy, P. Lentz, I. Kiricsi: Appl. Catal. B, 17 (1998) 157.

88 B. Coq, J.M. Cognion, F. Figuéras, D. Tournigant: J. Catal., 141 (1993) 21.

89 W. Juszczyk, A. Malinowski, Z. Karpinski: Appl. Catal. A, 166 (1998) 311.

90 B.S. Ahn, S.G. Jeon, H. Lee, K.Y. Park, Y.G. Shul: Appl. Catal. A., 193 (2000) 87.

91 M. Bonarowska, A. Malinowski, W. Juszczyk, Z. Karpinski: Appl. Catal. B, 30 (2001) 187.

92 M. Makkee, A. Wiersma, E.J.A.X. Sandt, H. van Bekkum, J.A. Moulijn: Catal. Today, 55 (2000) 125.

93 S. Ordonez, M. Makkee, J.A. Moulijn: Appl. Catal. B, 29 (2001) 13.

94 R. Ohnishi, W-L. Wang, M. Ichikawa: Appl. Catal. A, 113 (1994) 29.

95 A. Wiersma, E.J.A.X. Sandt, M. Makkee, P.P. Luteijn, H. van Bekkum, J.A. Moulijn: Catal. Today, 27 (1996) 257.

96 E.J. Creyghton, M.H.W. Burgers, J.C. Jansen, H. van Bekkum: Appl. Catal. A, 128 (1995) 275.

97 B. Coq, G. Ferrat, F. Figueras: React. Kinet. Catal. Lett., 27 (1985) 157.

98 B. Coq, G. Ferrat, F. Figueras: J. Catal., 101 (1986) 434.

99 P. Bodnariuk, B. Coq, G. Ferrat, F. Figueras: J. Catal., 116 (1989) 459.

100 S.T. Srinavas, L. Jhansi Lakshmi, N. Lingaiah, P.S. Sai Prasad, P. Kanta Rao: Appl. Catal. A, 135 (1996) L201.

101 F. Medina, P. Salagre, J.L.G. Fierro, J.E. Sueiras: Appl. Catal. A, 99 (1993) 115.

102 R.B. LaPierre, L. Guczi, W.L. Kranich, A.H. Wiess: J. Catal., 52 (1978) 218.

103 A.R. Suzdorf, S.V. Morozov, N.N. Anshits, S.I. Tsiganova, A.G. Anshits: Catal. Lett., 29 (1994) 49.

104 G. Tavoularis, M.A. Keane: J. Mol. Catal. A, 142 (1999) 187.

105 N. Lingaiah, Md. A. Uddin, A. Muto, T. Iwamoto, Y. Sakata, Y. Kusano: J. Mol. Catal. A, 161 (2000) 157.

106 Y. Cesteros, P. Salagre, F. Medina, J.E.Sueiras: Appl. Catal. B, 22 (1999) 135.

107 Y. Cesteros, P. Salagre, F. Medina, J.E.Sueiras: Appl. Catal. B, 25 (200) 213.

108 F. Gioia, F. Murena: J. Hazard. Mat., 57 (1998) 177.

109 F. Murena, F. Gioia: J. Hazard. Mat., 60 (1998) 271.

110 F. Murena: J. Hazard. Mat. B, 75 (2000) 49.

111 N. Couté, J. Richardson: Appl. Catal B, 26 (2000) 217.

112 H. Beyer, I. Bica, P.A. Jacobs: Magy. Kém. Foly., 83 (1977) 34.

113 P.A. Jacobs, H. Beyer: J. Phys. Chem., 83 (1979) 1174.

114 W.C. Conner, J.F. Falcone: Chem. Rev., 95 (1995) 759.

115 Z. Kónya, I. Hannus, I. Kiricsi: Stud. Surf. Sci. Catal., 105 (1997) 1509.

116 I. Hannus, I.I. Ivanova, G. Tasi, I. Kiricsi, J. B.Nagy: Stud. Surf. Sci. Catal., 84 (1994) 1123.

117 S.Y. Kim, H.C. Choi, O.B. Yanga, K.H. Lee, Y.G. Kim: J. Chem. Soc. Chem. Comun. (1995) 2169.

ACKNOWLEDGEMENT

I am deeply grateful to so many people for their help with my Ph.D.

Firstly, I owe a great dept to my supervisor to Prof. Imre Kiricsi for his indispensable patience and help. My grateful thanks to him for both theoretical and practical encouragement and teaching that I have received from him during the years that I spent working in his department.

I would also like to gratefully acknowledge Dr. János Halász who encouraged me in my first steps towards catalytic research and offered to help me on my scientific way.

I gratefully acknowledge the valuable services of Dr. István Pálinkó, who gave me so much useful advice. Without his brilliant editing pen my publications and thesis could not have assumed their form.

I would also like to thank Dr. Zoltán Kónya for his invaluable help. I am grateful for our conversations that helped me extend my horizons and gave me the strength to overcome both theoretical and practical obstacles arising in my work.

I have had the great advantage of having access to work of Mrs. Katalin Barna (XRD and TG measurements), Mrs. Anikó Márkus (literature works) and Mr. Csaba Asbóth (glass works). I thank them for this.

My thanks are due, too, to the whole of the Department of Applied and Environmental Chemistry for their support and friendship.

I gratefully acknowledge Prof. László Guczi, Prof. Zoltán Schay (at Department of Surface Chemistry Research Center, Hungarian Academy of Sciences), Prof. János B.Nagy (at Laboratoire de RMN, Facultes Universitaires Notre-Dame de la Paix, Namur, Belgium) and Prof. Fujio Mizukami (at NIMC, Surface Chemistry Department, Molecular Recognition Laboratory, Tsukuba, Japan) for having possibility to cooperate with them.

I would also like to thank Phoenix Rubber Industrial Ltd. and particularly the head of Compound Development and Technical Department Mrs. Zsuzsa Seregély for the support I have received from her in finishing my Ph.D. thesis at my work place.

Finally, many thanks to my family, friends and colleges for the tremendous support they gave me during the writing of my thesis.